PREPARATION OF CHITOSAN MODIFIED MMT/CHITOSAN COMPOSITE FILMS

WANDEE ANGKURA
SEKSAN SITTHICHAINAT

A Special Project Submitted in Partial Fulfillment of
the Requirements for the Degree of Bachelor of Science
Center for International Studies, Faculty of Science
King Mongkut's Institute of Technology Ladkrabang
Academic Year 2007

Title of Special Project	Preparation of Chitosan Modified MMT/Chitosan Composite Films
Student Names	Miss Wandee Angkura I.D. 47050591
	Mr. Seksan Sitthichainat I.D. 47050595
Department	Center for International Studies
Program	Polymer Science and Technology
Academic Year	2007
Special Project Advisors	Asst. Prof. Dr. Pathavuth Monvisade
	Asst. Prof. Dr. Punnama Siriphannon
	Asst. Prof. Dr. Chonlada Ritvirulh

ABSTRACT

Chitosan modified MMT/chitosan (CHI-MMT/chitosan) composites were prepared using 1, 2, 3% of MMT and then coated on filter paper by spin coating technique. The chitosan and CHI-MMT/chitosan composites were characterized by FTIR. Various sequences of coating layers were performed, i.e. MMMM, CCCC, CMMC and MMCC (M= CHI-MMT/chitosan composite, C=chitosan solution). The coated filter papers were characterized by XRD, XRF, and SEM/EDS. The continuous phases of CHI-MMT/chitosan impregnate in the space among the cellulose fibrous. However, the particles containing silicon could be observed in SEM micrographs of all coated filter papers. The results of contact angle indicated that CCCC gave lower wettability but higher water permeability than MMMM. However, MMCC could improve both water wettabiity and permeability. Moreover, preliminary study of moisture permeability of coated filter paper showed the lowering of permeability in comparison with filter paper.

ACKNOWLEDGEMENT

The authors would like to take this opportunity to express sincere thanks to their teachers and people who gave useful advice and full support in this research.

The authors wish report in the special project submitted in partial fulfillment of the requirement for the Bachelor Degree of Science in Polymer Science and Technology Program, Center for International Studies, Faculty of Science at King Mongkut's Institute of Technology Ladkrabang to express them deep gratitude to Asst. Prof. Dr. Punnama Siriphannon, Asst. Prof. Dr. Pathavuth Monvisade and Asst. Prof. Dr. Chonlada Ritvirulh their the special project advisor, for valuable guidance, attraction, and encouragement throughout this research. It goes without saying to the special project of polymer committees i.e., Asst. Prof. Dr. Suparat Rukchonlatee and Assoc. Prof. Dr. Ittipol Jangchud who are the teachers in our department. Then, we just got more knowledge in this topic. They are reading and criticizing the manuscript.

Special thanks go to staffs in Scientific Instruments Service Centre for their helps in the analysis instruments in XRD and XRF, FTIR instrument at the 5th floor of Scientist Building, at the Department of Chemistry, and computer room at Chulabhon 2 building 2, 2nd floor in Faculty of Science at King Mongkut's Institute of Technology Ladkrabang. SEM and EDS were analyzed at Scientific and Technological Research Equipment Centre, Chulalongkorn University, Bangkok. The last one, contact angle (θ) was measure at the Royal Forest Department, Bangkok.

We also would like to give the special thanks to all of them friends for international programs studies and the other people that have been helping and encouraging us while studying at King Mongkut's Institute of Technology Ladkrabang.

The last but not least, we would like to express them deepest appreciation to our families that are the most importance in our lives forever.

Miss. Wandee Angkura

Mr. Seksan Sitthichainat

TABLE OF CONTENTS

TABLE OF CONTENTS (CONTINUED)

LIST OF TABLES

LIST OF FIGURES

Chapter 1

Introduction

1.1 Introduction

In recent years, montmorillonite (MMT) has attracted in the both academic and industrial fields because of its high aspect ratio of silicate layers, high surface area and the wide applications in the polymer composites. As is well-known, polymer-clay composites are materials of increasing interest because of their structural or functional behavior. For instance, interesting electrical and electrochemical properties of poly (ethylene oxide)-smectites have been extensively reported. The opportunity to combine at the metric level clays and a natural polymer (biopolymer) such as chitosan also appears as an attractive way to develop new organic-inorganic hybrid materials provided with properties that are inherent to both types of components.

Common organoclays have been used as inorganic fillers for the conventional polymer composites to reduce the cost or to give them special properties such as modulus, hardness, thermal stability, opacity and brightness, etc. one types of clay is aluminosilicates, which have a sheet like (layered) structure, and consist of silica SiO_4 tetrahedra bonded to alumina AlO_6 octrahedra in a variety of ways. A 2:1 ratio of the tetrahedral to the octrahedra results in smectite clays, the most common of which is MMT. Depending on the precise chemical composition of the clay, the sheet bear a charge on the surface and edges, this charge being balanced by couterions, which reside in part in the inter-layer spacing of the clay. The thickness of the layer (platelets) is of order of 1 nm. The clay platelets are truly particulate. The chitosan was use for intercalated into MMT for improve the specific properties is a long chain aminelor aliphatic amine polymer. The first, chitosan layer is adsorbed through a

cationic exchange procedure, while the second layer is adsorbed in the acetate salt form. Because the deintercalation of the biopolymer is very difficult, the $-NH_3^+Ac^-$ species belonging to the chitosan second layer act as anionic exchange sites and, in this way, such composites become suitable systems for the detection of anions.

In this study, the CHI-MMT/chitosan composite (organoclay) films made from MMT (reinforcement) and chitosan (polymer matrix) has been developed. MMT and chitosan was mix using mechanical stirrer. Concerning synthetic polymers, improve the properties of biodegradable polymer matrix. By varying the weight ratio of MMT to chitosan and the order layers of clay on filter paper. The physical and morphology characteristics of CHI-MMT/chitosan composite films are investigated in order to the characterization by using XRD, XRF, FTIR, and SEM/EDS. The contact angle measurement and preliminary permeability test were investigated.

1.2 Objectives

1.2.1 To study on the preparation of CHI-MMT/chitosan composite films.

1.2.2 To study effect of MMT content on physical and morphology properties.

1.3 Scope of Study

1.3.1 Preparation of CHI-MMT/chitosan with different MMT contents, i.e., 1%, 2%, and 3% weights.

1.3.2 Characterization of composite films using various techniques, i.e., XRD, XRF, FTIR, and SEM/EDS. The contact angle measurement and preliminary permeability test were investigated.

1.4 Expected Results

1.4.1 The CHI-MMT/chitosan composite films are prepared by various MMT contents in order to obtain the most efficient content.

1.4.2 The knowledge from this project can be improving properties of composite films that made from CHI-MMT/chitosan composite films in the future.

Chapter 2

Theory and Literature Reviews

2.1 Clay and Clay Modifications [1,2]

Clay is a naturally occurring material composed primarily of fine-grained minerals, which show plasticity through a variable range of water content, and which can be hardened when dried or fired. Clay deposits are mostly composed of clay minerals (phyllosilicate minerals), minerals which impart plasticity and harden when fired or dried, and variable amounts of water trapped in the mineral structure by polar attraction. Organic materials which do not impart plasticity may also be a part of clay deposits.

Clay minerals are typically formed over long periods of time by the gradual chemical weathering of rocks (usually silicate-bearing) by low concentrations of carbonic acid and other diluted solvents. These solvents (usually acidic) migrate through the weathering rock after leaching through upper weathered layers. In addition to the weathering process, some clay minerals are formed by hydrothermal activity. Clay deposits are formed in place as residual deposits, but thick deposits usually are formed as the result of a secondary sedimentary deposition process after they have been eroded and transported from their original location of formation. Clay deposits are typically associated with very low energy depositional environments such as large lake and marine deposits.

2.1.1 Physical Characteristics of Clay [3]

1 Clay minerals tend to form microscopic to sub microscopic crystals.

2 They can absorb water from simple humidity changes.

3 When mixed with limited amounts of water, clays become plastic and are able to be molded and formed as children's clay.

4 When water is absorbed, clays will often expand as the water fills the spaces between the sacked silicate layers.

5 Due to the absorption of water, the specific gravity of clays is high variable and is lowered with increased water content.

6 The hardness of clays is difficult to determine due to the microscopic nature of the crystals, but the hardness is usually between 2 and 3 and many clays give a hardness of 1 in field tests.

7 Clays tend to form weathering and secondary sedimentary processes with only a few examples of clays forming in primary igneous or metamorphic environments.

8 Clays are rarely found separately and are usually mixed not only with other clays but with microscopic crystals of carbonates, feldspars, micas and quartz.

2.1.2 Clay Classification [3,4,5]

Clay minerals are divided into four major groups. These are the important clay mineral groups:

1) The kaolinite group

This group has three members (kaolinite, dickite and nacrite) and a formula of $Al_2Si_2O_5(OH)_4$. The different minerals are polymorphs, meaning that they have the same chemistry but different structures (polymorph = many forms). The general structure of the kaolinite group is composed of silicate sheets (Si_2O_5) bonded to aluminum oxide/hydroxide layers ($Al_2(OH)_4$) called gibbsite layers. The silicate and gibbsite layers are tightly bonded together with only weak bonding.

Uses: In ceramics, as a filler for paint, rubber and plastics and the largest use is in the paper industry that uses kaolinite to produce a glossy paper such as is used in most magazines.

2) The montmorillonite (MMT)/smectite group

This group was composed of several minerals including pyrophyllite, talc, vermiculite, sauconite, saponite, nontronite and MMT they differ mostly in chemical content. The general formula is $(Ca, Na, H)(Al, Mg, Fe, Zn)_2(Si, Al)_4O_{10}(OH)_2 \cdot xH_2O$, where x represents the variable amount of water that members of this group could contain. Talc's formula, for example, is $Mg_3Si_4O_{10}(OH)_2$. The gibbsite layers of the kaolinite group can be replaced in this group by a similar layer that is analogous to the oxide brucite, $(Mg_2(OH)_4)$. The structure of this group is composed of silicate layers sandwiching a gibbsite (or brucite).

Uses: Are many and include a facial powder (talc), filler for paints and rubbers, an electrical, heat and acid resistant porcelain, in drilling muds and as a plasticizer in molding sands and other materials.

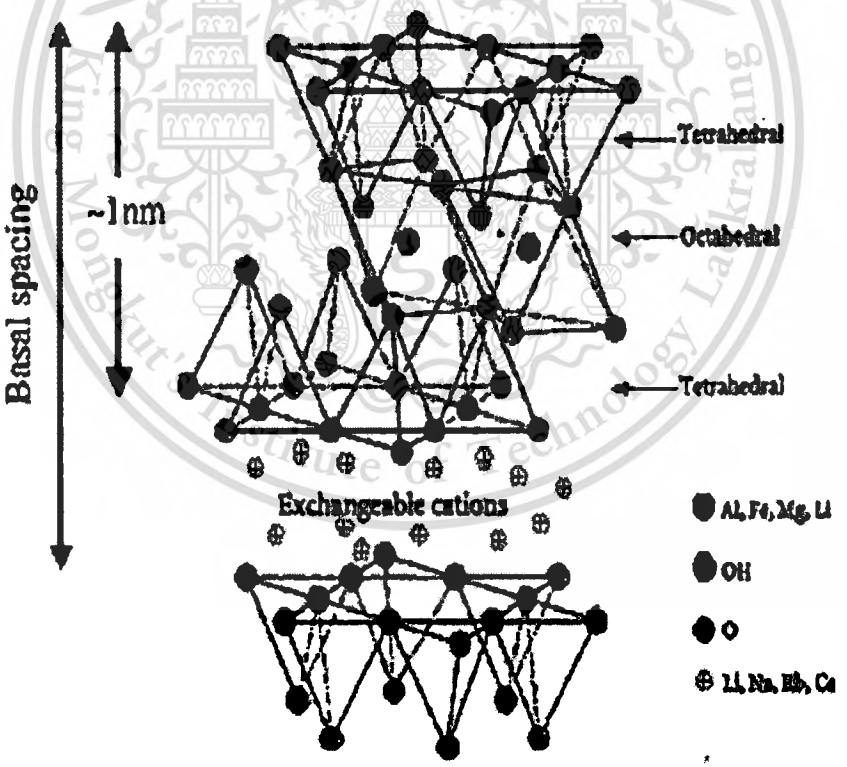

Figure 2.1 Structure of MMT

3) The illite (or the clay-mica) group

This group is basically a hydrated microscopic muscovite. The mineral illite is the only common mineral represented, however it is a significant rock forming mineral being a main component of shales and other argillaceous rocks. The general formula is $(K, H)Al_2(Si,Al)_4O_{10}(OH)_2 - xH_2O$, where x represents the variable amount of water that this group could contain. The structure of this group is similar to the MMT group with silicate layers sandwiching a gibbsite-like layer. The variable amounts of water molecules would lie as well as the potassium ions.

Uses: A common constituent in shales and is used as a filler and in some drilling muds.

4) The chlorite group

This group is not always considered a part of the clays and is sometimes left alone as a separate group within the phyllosilicates. It is a relatively large and common group although its members are not well known.

The term chlorite is used to denote any member of this group when differentiation between the different members is not possible. The general formula is $X_{4-6}Y_4O_{10}(OH,O)_8$. The X represents either aluminum, iron, lithium, magnesium, manganese, nickel, zinc or rarely chromium. The Y represents either aluminum, silicon, boron or iron but mostly aluminum and silicon. The gibbsite layers of the other clay groups are replaced in the chlorites by a similar layer that is analogous to the oxide brucite. The structure of this group is composed of silicate layers sandwich with a brucite or brucite-like layer, however, in the chlorites, there is an extra weakly bonded in brucite layer.

Uses: No industrial uses.

Some minerals listed above (specifically chlorite, pyrophyllite and talc) as belonging to one of the clay groups are often excluded by some minerologists. Usually the reason is that their crystal size and character due not consistently conform to those parameters that define clay. Such minerals are listed here more for their structural similarities, however all three minerals are quite often found associated with and do behave like clays occasionally.

2.1.3 Clay Modifications [4]

One important consequence of the charged nature of the clays is that they are generally highly hydrophilic species and therefore naturally incompatible with a wide range of polymer types. A necessary prerequisite for successful formation of polymer-clay nanocomposites is therefore alteration of the clay polarity to make the clay 'organophilic'. An organophilic clay can be produced from a normally hydrophilic clay by ion exchange with an organic cation such as an alkylammonium ion. For example, in montmorillonite, the sodium ions in the clay can be exchanged for an amino acid such as 12-aminododecanoic acid (ADA):

$$Na^{+}\text{-CLAY} + HO_2C\text{-R-}NH_3^{+}Cl^{-} \rightarrow .HO_2C\text{-R-}NH_3^{+}\text{-CLAY} + NaCl \qquad (1)$$

The way in which this is done has a major effect on the formation of particular nanocomposite product forms and this is discussed further below. Although the organic pre-treatment adds to the cost of the clay, the clays are nonetheless relatively cheap feedstocks with minimal limitation on supply. Montmorillonite is the most common type of clay used for nanocomposite formation; however, other types of clay can also be used depending on the precise properties required from the product. These clays include hectorites (magnesiosilicates), which contain very small platelets, and synthetic clays (e.g. hydrotalcite), which can be produced in a very pure form and can carry a positive charge on the platelets, in contrast to the negative charge found in montmorillonites.

2.2 Chitin and Chitosan [6,7,8,9,10]

Chitin is not exactly a household word, but most are familiar with its source. It is found naturally in the shells of crustaceans, such as crab, shrimp and lobster, as well as in the exoskeleton of marine zoo-plankton, including coral and jellyfish. Insects, such as butterflies and ladybugs, have chitin in their wings. And the cell walls of yeast, mushrooms and other fungi also contain this natural substance.

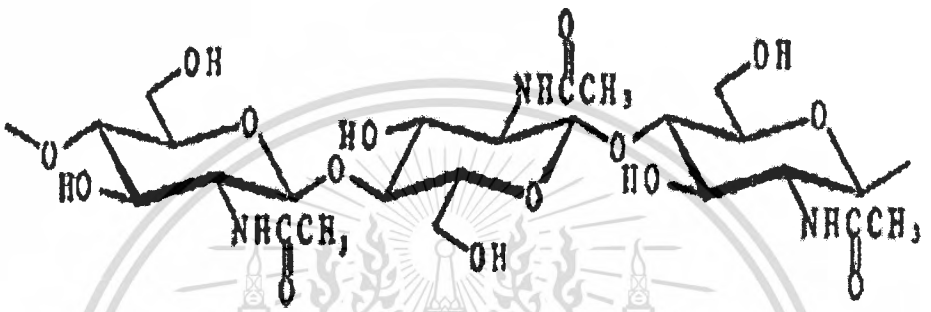

Figure 2.2 Structure of chitin

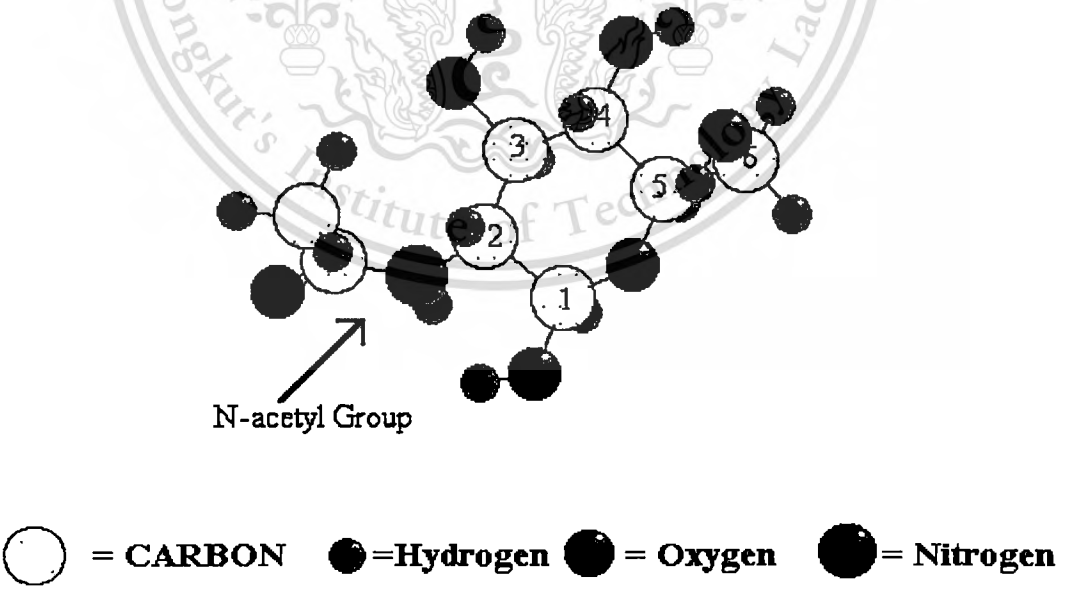

Figure 2.3 Structure of chitin that show n-acetyl group

Chitin was first sound in mushrooms in 1811s by Professor Henri Braconnot while he was Professor of Natural History and Director of the Botanical Gardens at the Academy of Sciences in Nancy, France. In the 1830s, it was isolated in insects and named chitin. Professor C. Rouget discovered chitosan in 1859, and over the next century, much fundamental research took place on these compounds. An intense interest in new applications grew in the 190s and early 1940s, as evidenced by almost 50 patents; however, the lack of adequate manufacturing facilities and competition from synthetic polymers hampered commercial development. Renewed interest in the 1970s was encouraged by the need to better utilize shellfish shells. Scientist worldwide began to chronicle the more distinct properties of chitin and its derivatives and understand the potential of these natural polymers. Since then, numerous research studies have been undertaken to find ways to use materials. Over the last 200 years, the exploration of chitosan taken to many difference forms. Several other researchers' continuto build on the original finding of Bracannot, discovering new use for chitin as they find different forms of it in nature.

Chitin and its derivatives have many properties that make them attractive for a wide variety of applications. Their anti-fungal and anti-viral properties make them particularly useful for biomedical applications, such as wound dressings, surgical sutures and as aids in cataract surgery and periodontal disease treatment. Chitin and chitosan are non-toxic and non-allergenic, so the body is not likely to reject these compounds as foreign invaders. Chitin's biodegradable and anti-fugal properties are a plus for environmental and agricultural uses.

Chitin is one of the three most abundant polysaccharides in nature, in addition to cellulose and starch. It ranks second to cellulose as the most plentiful organic compound on earth. Cellulose and starch are key carbohydrates which plants use as a food source and to build cell walls. In addition, they have widespread use in the industry. Researchers and entrepreneurs see similar potential for chitin.

Chitosan is a linear polysaccharide composed of randomly distributed β-(1-4)-linked D-glucosamine (deacetylated unit) and N-acetyl-D-glucosamine (acetylated unit). It has a number of commercial and possible biomedical uses. Chitosan is produced commercially by deacetylation of chitin , which is the structural element in the exoskeleton of crustaceans (crabs, shrimp, etc.). The degree of

deacetylation (%DA) can be determined by NMR spectroscopy, and the %DA in commercial chitosans is in the range 60-100 %.The amino group in chitosan has a pKa value of ~6.5, thus, chitosan is positively charged and soluble in acidic to neutral solution with a charge density dependent on pH and the %DA-value. In other words, chitosan is bioadhesive and readily binds to negatively charged surfaces such as mucosal membranes. Chitosan enhances the transport of polar drugs across epithelial surfaces, and is biocompatible and biodegradable. Purified qualities of chitosans are available for biomedical applications.

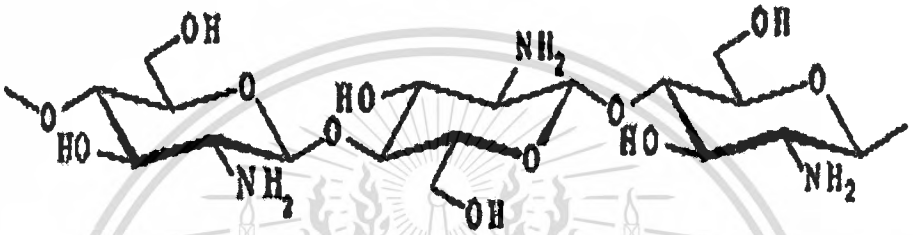

Figure 2.4 Structure of chitosan

2.2.1 Preparation of chitin and Chitosan [11]

At present time, the easiest and famous method was suggested by Muzzarelli, which the decalcification was carried out by soaking the crushed crab shells in HCl at room temperature. After that, NaOH solutions is used to remove the proteins (deproteination), and washed to neutral. The deacetylation of chitin is achieved by soaking the chitin samples in NaOH solutions of various concentrations.The decolorization in $KMnO_4$ and oxalic acid with autoclave or sunshine.

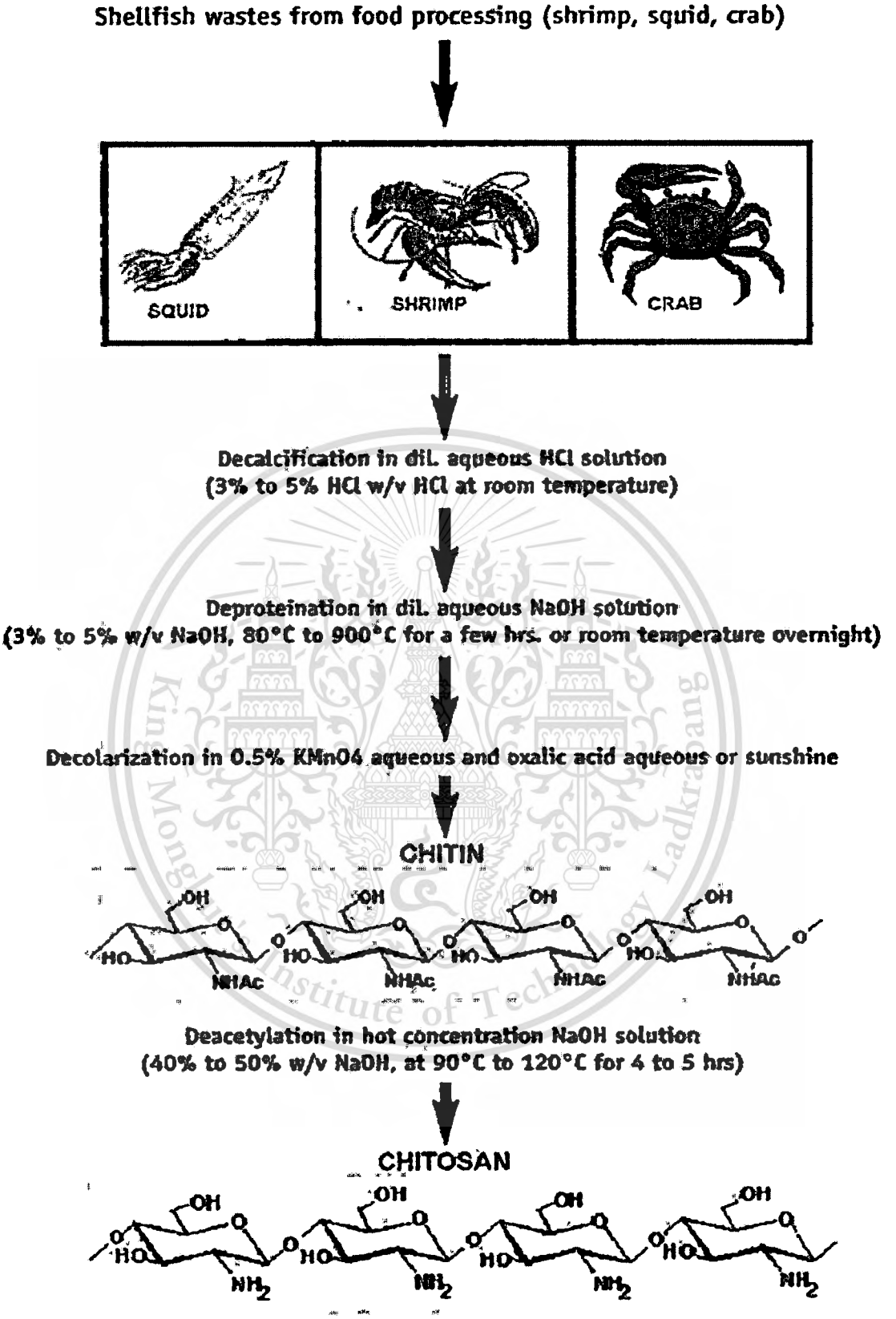

Figure 2.5 Preparation of chitin and chitosan

2.2.2 Characterization [12]

Both chitin and chitosan are naturally biodegrable and nontoxic. Chitosan can be described in general by following parameters: degree of deacetylation (%), dry matter (%), ash (%), protein (%), viscosity in centipoise, intrinsic viscosity (η_{sp}/C), molecular weight (g/mol), and turbidity (NTU units). All these parameters can be adjusted to the application chitosan is being used for.The main parameters that influence on the product properties is as mentioned above, the degree of deacetylation and viscosity. The deacetylation is very important to get a soluble product. But it is not only the degree of deacetylation that influence on the solubility. The distribution of the acetyl groups is also important. Moreover, viscosity can be adjusted to each application, by controlling process parameters.

2.2.3 Application [12,13]

Chitosan is unique, with a polyamine character which makes it soluble (at acid pH), positively charged, different viscosity and easily modified chemically. These properties confer upon chitosan potential applications in nutritional uses, food, biomedicine, skin and hair care, environment and agriculture, and others.

2.3 Nanocomposite [14]

Nanocomposites are a new class of composites, which are particle-filled polymers for which at least one dimension of the dispersed particles, is in the nanometer range. One can distinguish three types of nanocomposites, depending on how many dimensions of the dispersed particles are in the nanometer range. When the three dimensions are in the order of nanometers, we are dealing with isodimensional nanoparticles, such as spherical silica nanoparticles obtained by *in situ* sol±gel methods or by polymerization promoted directly from their surface, but also can include semiconductor nanoclusters and others. When two dimensions are in the nanometer scale and the third is larger, forming an elongated structure, we speak about nanotubes or whiskers as, for example, carbon nanotubes or cellulose whiskers which are extensively studied as reinforcing nanofillers yielding materials with exceptional properties. The third type of nanocomposites is characterized by only one dimension in the nanometer range. In this case the filler is present in the form of sheets of one to a few nanometer thick to hundreds to thousands nanometers long. This family of composites can be gathered under the name of polymer-layered crystal nanocomposites, and their study will constitute the main object of this contribution. These materials are almost exclusively obtained by the intercalation of the polymer (or a monomer subsequently polymerized) inside the galleries of layered host crystals. There is a wide variety of both synthetic and natural crystalline fillers that are able, under specific conditions, to intercalate a polymer.

Amongst all the potential nanocomposite precursors, those based on clay and layered silicates have been more widely investigated probably because the starting clay materials are easily available and because their intercalation chemistry has been studied for a long time. Owing to the nanometer-size particles obtained by dispersion, these nanocomposites exhibit markedly improved mechanical, thermal, optical and physico-chemical properties when compared with the pure polymer or conventional (microscale) composites as firstly demonstrated by Kojima and coworkers for nylon±clay nanocomposites. Improvements can include, for example, increased moduli, strength and heat resistance, decreased gas permeability and flammability.

2.3.1 Processing Conditions

The traditional routes to prepare nanocomposites using layered compounds as reinforcement, especially clays, can be summarized as follows:

1) *in situ* polymerization

Polymer is formed (initiation of polymerization by heating or radiation or by diffusion) between the layers by swelling the layer hosts within the liquid monomer or monomer solution.

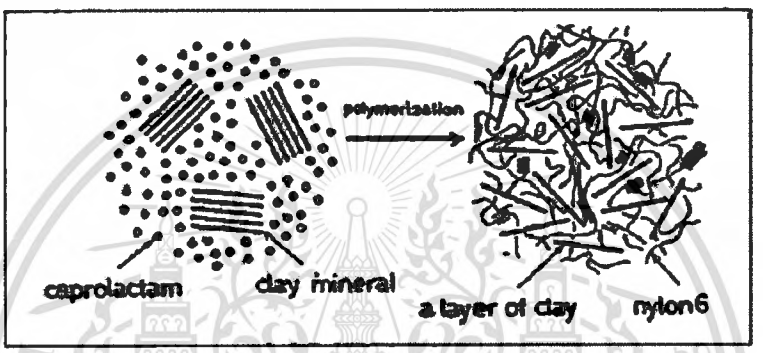

Figure 2.6 Schematic illustrations for synthesis of nylon-6/clay nanocomposites

2) Melt intercalation

This method, an environmentally benign one, uses all types of polymers as well as being compatible with practicing polymer industrial processes such as injection molding, being the most popular procedure to prepare nanocomposites for industrial applications. In this method, polymers, and layered hosts are annealed above the softening point of the polymer.

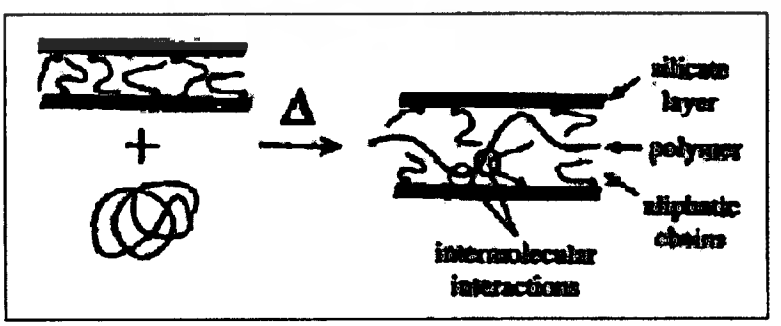

Figure 2.7 Schematic depicting the intercalation process between a polymer melt and an organic modified layered silicate

3) Intercalation of prepolymer from solution

The layered host is to be swelled in a solvent (water, toluene, etc.) followed by its mixture with polymer or prepolymer, whereby the chains of the latter intercalate while displacing the solvents used for swelling. Polymer layered nanocomposite results when the solvent within the interlayer is removed.

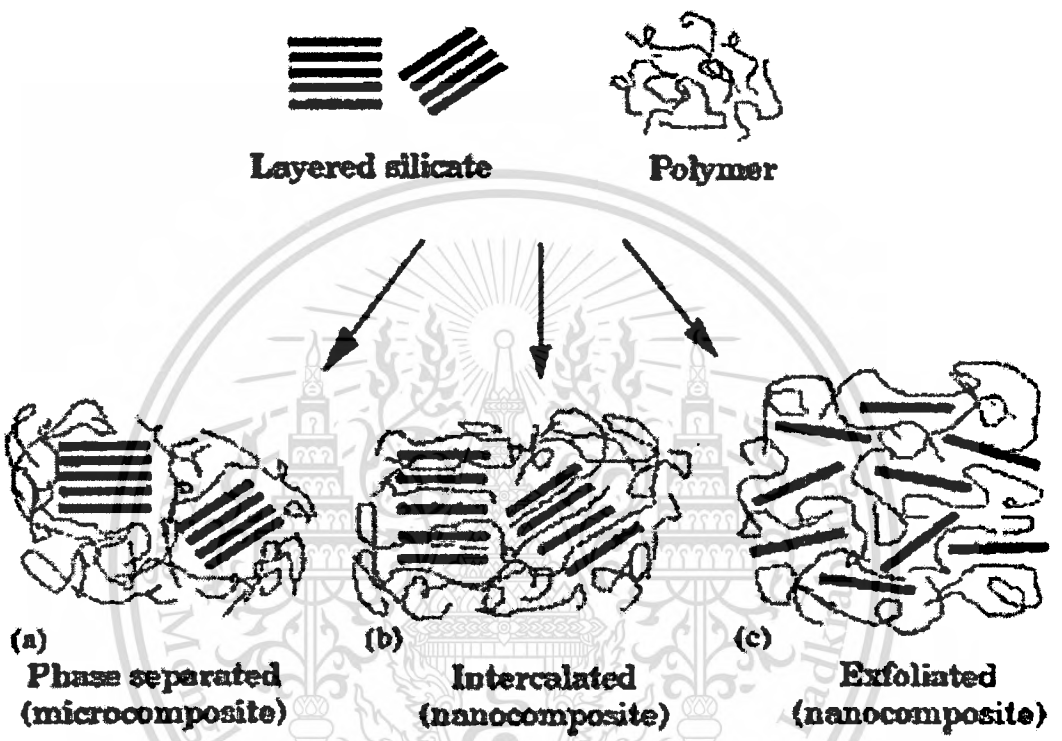

Figure 2.8 Scheme of different types of composite arising from the interaction of layered silicates and polymers: (a) phaseseparated microcomposite; (b) intercalated nanocomposite and (c) exfoliated nanocomposite.

2.4 Literature Reviews

Darder M, Collila M, and Ruiz-Hitzky E, [15], 2003, studied on the intercation of the cationic biopolymer chitosan in Na^+ - montmorillonite, providing compact and robust three-dimentional nanocomposites with functional properties. CHN chemical analysis, X-ray diffraction, Fourier transform infrared spectroscopy, scanning transmission electron microscopy, energy-dispersion X-ray analysis, and thermal analysis have been employed in the characterization of the nanocomposites, confirming the absorption in mono- or bilayers of chitosan chains depending on the relative amount of chitosan with respect to the cationic exchange capacity of the clay. The first chitosan layer is adsorbed through a cationic exchange procedure, while the second layer is adsorbed in the acetate salt form. Because the deintercalation of the biopolymer is very difficult, the $-NH_3^+$ Ac- species belonging to the chitosan second layer act as anionic exchange sites and, in this way, such nanocomposites become suitable systems for the detection of anionic.

Adriana Czimerova, L'ubos Jankovic, and Jaraj Bujdak, [16], 2004, concerned in the adsorption of a cationic dye, methylene blue (MB), on the surface of montmorillonite. The montmorillonite samples, saturated with various inorganic cations (mono-, bi-, and trivalent, including those of transition metals), were used. Influence of the exchangeable cations on the MB aggregation was tested. It was found that the available surface area and some phenomena relate to the parameter, such as swelling, tactoic formation, did not significantly affect dye cation aggregation under the condition used. However, layer charge distribution, as an intrinsic property of clay surface, may not be the only parameter that significantly effects the dye aggregation. The presence of large alkali metal cations (K^+, Rb^+, and Cs^+) or NH_4^+, which are less mobile and partially fixed on the clay surface, may significantly influenced an ion exchange reaction. The lower mobility of these cations may lead to incomplete ion exchange.

Darder M, Lopez-Blanco M, Aranda P, Leroux F, and Ruiz-hitzky E, [17], 2005, concerned in synthesization of [Zn_2Al] LDH (layered double hydroxide). The "coprecipitation" or "co-organized assembly" method has been successfully employed for the intercalation of such polysaccharides within the [Zn_2Al] LDH. The "reconstruction" procedure from the calcined LDH in the presence of the anionic polysaccharides only resulted in a partial intercalation of the organic guest. Particular efford was devoted to the study of E-carageenan-[Zn_2Al] systems. XRD clearly shows the interaction of alginate, pectin, and E-carrageenan between the layers of Zn_2Al LDH. The alginate and pectin are intercalated as a monolayer of the biopolymer, whereas ι-carrageenan showing a higher ΔdL is intercalated as a bilayeror most likely as a double helix. It is difficult at this stage of the investigation to confirm this last conformation. IR, EDX, and C-NMR techniques corroborate that the interaction in always driven by electrostatic interactions between the negatively charged groups of the biopolymer and the positively charged LDH layers.

Darder M, Colilla M, and Ruiz-hitzky E, [18], 2005, the objective was the application of biopolymer-clay nanocomposites in the development of electrochemical sensor for the potentionmetric determination of anionic species. Since chitosan-montmorillonite nanocomposites exhibited good functional and mechanical properties, they are employed in the construction of bulk-modified sensors for the detection of anions. These nanocomposites were combined with graphite particles to provide the system with electronic conductivity. Besides, the developed electrodes ware provided of low environment impact, and these devices are successfully applied in the potentiometric determination of several anions.Showing a higher selectivity towards monovalent rather than to di- or trivalent anions and the best potentiometric response towards nitrate ions. Moreover, chitosan- montmorillonite nanocomposites appeared as excellent materials for the development of bulk-modified potentiometric sensor for the anionic detection in aqueous samples.

Li Wang, Aiqin Wang, [19], 2007, the nanocomposites were characterized by FTIR, XRD and SEM. Adsorption of Congo red (CR) anionic dye from aqueous solution onto *N,O*-CMC–MMT was studied. The results showed that the nanocomposite with the molar ratio of *N,O*-CMC to MMT of 5:1 exhibited the higher adsorption capacity. The results of adsorption behaviors of CR on *N,O*-CMC–MMT indicated that all the adsorption processes followed the pseudo-second-order and the Langmuir isotherm, respectively. Novel *N,O*-CMC–MMT nanocomposites were synthesized by intercalation reaction between *N,O*-CMC and MMT in distilled water. Adsorption tests of CR dye on *N,O*-CMC–MMT nanocomposites were carried out and the results obtained from this study show that the nanocomposite with the molar ratios of *N,O*-CMC to MMT of 5:1 exhibited the higher adsorption capacity. The kinetic and isotherm studies indicated that the pseudo-second-order model and the Langmuir model well described the adsorption equilibrium of CR on *N,O*-CMC–MMT nanocomposite. As a novel nanocomposite material, *N,O*CMC– MMT is a promising biosorbent for dye removal from CR dye wastewater.

Darder Kun-Ho Liu, Ting-Yu Liu, San-Yuan Chen, Dean-Mo Liu, [20], 2007, study on the nanohydrogel with 2 wt.% MMT achieved a mechanically reliable and practically desirable pulsatile release profile and excellent anti-fatigue behavior, compared with that of the pure CS. A CS–MMT nanohydrogel responsive to electrostimulation was successfully prepared and systematically characterized in terms of crystallinity, anti-fatigue property and drug release behavior. The exfoliated silica sheets act as cross-linkers to form a strong network structure between the CS and MMT. Under an applied voltage, the drug release behavior was strongly influenced by the concentration of MMT, which affected the cross-linking density of the nanohydrogels. Vitamin B_{12} displays pseudo-zeroorder release kinetics and the release mechanism shifted from being diffusion-controlled to being swelling-controlled mode when a low MMT content (1 wt.%) was added. However, with an MMT content exceeding 1 wt.%, both the diffusion exponent *n* and the responsiveness to electrical stimulation were decreased. Furthermore, the resulting nanostructure of the nanohydrogels can be successfully manipulated to keep the pulsatile release.

Chapter 3

Research Methodology

3.1 Materials

1. Chitosan of %DD = 82.5, which is obtained from deacetylation of chitin, ELAND Corporation, Ltd.
2. Mac-gel montmorrilonite (MMT), Thai Nippon Chemical Industry, Ltd.
3. AR grade of glacial acetic acid (HAc) used as solvent of chitosan, CARLO ERBA, Ltd.
4. Commerce grade sodium hydroxide (NaOH), CARLO ERBA, Ltd.

3.2 Apparatus

1. Mesh
2. Mortar
3. Glassware
4. Desiccator
5. Incubator
6. Micrometer
7. Plastic box, size 16 cm x 22 cm x 12 cm
8. Filter paper, No.2, Toyo Roshi Kaisha, Ltd.
9. Water bath, Memmert, Fisher Scientific Ltd.
10. Peristaltic pump, V 77120-52, Cole Parmer Ltd.
11. Spin coater, Buehler Beta Grinder polisher, Ltd.
12. Chemical dryers, Isotemp, Fisher Scientific Ltd.
13. Weighing apparatus, TC-254, Denver Instrument Ltd.
14. Mechanic stirrer, Euro-ST B, Ika Laboratory Staufen Ltd.

15. Drop shape analysis system, DSA100, KRÜSS GmbH, Ltd.
16. Flexible tubing for peristaltic pump, R3603, Cole Parmer Ltd.
17. X-ray diffractometer (XRD), D 8 Advance, Bruker AG Ltd.
18. Brook field viscometer, RVT, Brook field Engineering Laboratories INC.
19. X-ray fluorescence spectrometry (XRF), SRS 3400, Bruker AG Ltd.
20. Fourier Transform infrared Spectrophotometer (FTIR), FTIR Spectrum GX, Perkin Elmer Ltd.
21. Uniaxial pressing, SSP-10A, Shimadzu Corporation Ltd.
22. Field emission scanning electron microscope (FESEM/EDS), JSM-5800LV, Jeol Ltd.
23. Ultrasonic Vibration, ULTRAsonik, Fisher Scientific Worldwide Ltd.

3.3 Preparation of CHI-MMT/Chitosan Composite Films

3.3.1 Preparation of Swelled MMT Solution

1. 25 g of MMT was dispersed into 3000 ml of distilled water and sonicated in ultrasonic for 2 hours.
2. The decant of the well disperse MMT mixture was allow to dry in the hot air oven at 60°C for 48 hours.
3. The MMT was ground with mortar and kept in desiccators. Then, the MMT powder was sieved by 400 meshes.
4. 2% v/v of acetic acid was added in 50 ml of distilled water in order to get the acetic solution.
5. Various MMT content, i.e., 1, 2, and 3% by weight was dispersed into the acetic acid solution and sonicated for 1 hour.
6. The pH of the mixture was adjusted to about 5 with 0.1M NaOH solution.

3.3.2 Preparation of Chitosan Solution

1. 2% v/v of acetic acid was added in 50 ml of distilled water in order to get the acetic solution.
2. 4 g of chitosan was slowly added into the acetic acid solution. The mixture was stirred by using mechanic stirrer (300 rpm) for 3 hours at 50°C in the water bath.
3. The pH of the mixture was adjusted to about 5 with 0.1M NaOH solution.

3.3.3 Preparation of CHI-MMT/Chitosan Composite Films

1. The chitosan solution was slowly added into the swelled MMT solution using peristaltic pump at flow rate of 0.83 ml/min. The mixture was stirred with mechanic stirrer (700 rpm) at 60°C in the water bath for 3 hours.
2. 30 ml of the mixture was coated on filter paper with 150 rpm of the spin coater. The order of coating layer and formulae were shown in figure 3.1 and table 3.1. The sample was allowed to dry for 24 hours.
3. The CHI-MMT/chitosan composite films were characterized using various techniques, i.e., XRD, XRF, FT-IR, and SEM/EDS.

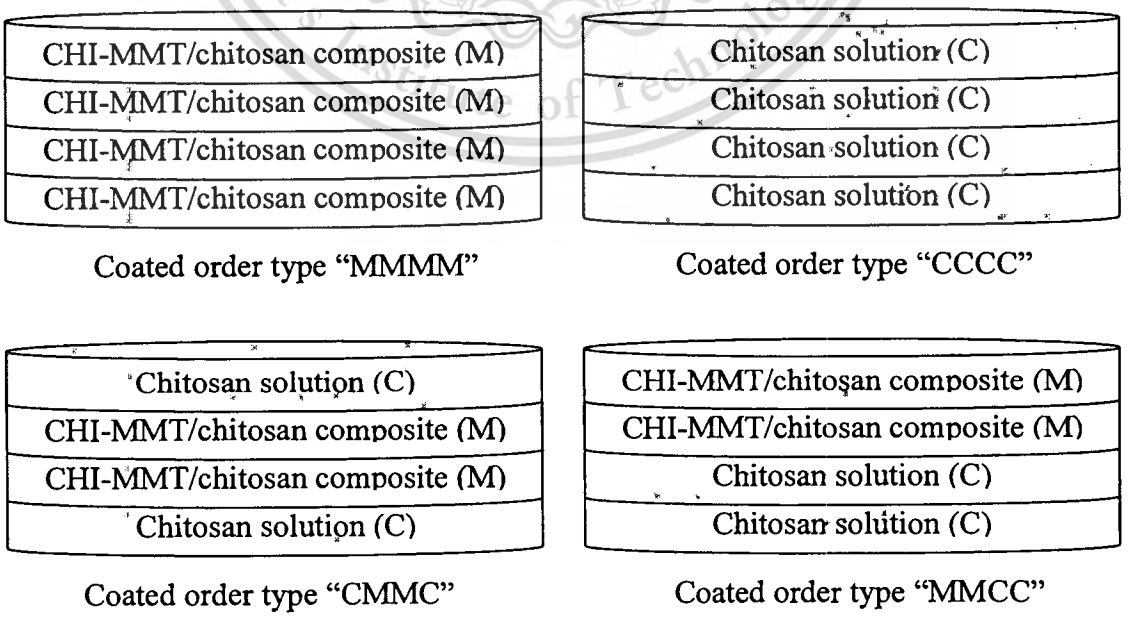

Figure 3.1 Schematic representation of coating layer

Table 3.1 The formulae of CHI-MMT/chitosan composite coated on filter paper

Sample No.	Percentage of MMT	Layer Arrangements Upper layer to lower layer
1	1	MMMM1
2	1	CMMC1
3	1	MMCC1
4	2	MMMM2
5	2	CMMC2
6	2	MMCC2
7	3	MMMM3
8	3	CMMC3
9	3	MMCC3
10	0	CCCC

3.4 Contact Angle Measurement

0.8 μL of distilled water was dropped on a smooth surface of CHI-MMT/chitosan composite coated on filter paper samples. The pictures and contact angle were recorded from 0 to 60 seconds.

3.5 Permeability Test

1. Two bottles were filled with anhydrous Na_2SO_3.
2. The lids of bottles were covered by filter paper and CHI-MMT/chitosan coated on filter paper, respectively.
3. The bottles were weighed and put in the hot air oven, containing water, at 95°C
4. The bottles were taken out and weighed daily for 4 days.
5. The moisture content could be calculated by the following equation:

$$\frac{Wt - Wi}{W_{Na_2SO_4}} \times 100 = \%\text{Moisture content/g of anhydrous } Na_2SO_4(t)$$

W_t = $(W_f + W_b + W_{Na_2SO_4})$ at each time

W_i = $(W_f + W_b + W_{Na_2SO_4})$ at initial

W_f = Weight of filter paper or coated filter paper

W_b = Weight of bottle and lid

$W_{Na_2SO_4}$ = Weight of anhydrous Na_2SO

3.6 Preliminary Characterization of CHI-MMT/Chitosan Composites

3.6.1 X-ray diffractometer (XRD)

X-ray diffraction (XRD, D8 advance, Bruker AG Ltd.) pattern was recorded using Cu Kα radiation (α = 15.4 nm) at a voltage of 30 kV and a current of 30 mA. (2 θ in 1° - 25°, step size 0.040°, and step time 0.5 second)

3.6.2 X-ray fluorescence spectrometry (XRFs)

The samples (0.5 g or 4x4 cm) of X-ray fluorescence spectrometry (XRFs, SRS 3400, Bruker AG Ltd.), were mixed with boric acid to determine the chemical composition of the samples.

3.6.3 Fourier Transform infrared Spectrophotometer (FTIR)

Samples (0.1 g) were grounded with KBr powder and compressed to be a pellet form using a uniaxial pressing. The samples were recorded using FT-IR (SpectrumGX, Perkin Elmer, Ltd.) and scanned from 4000-400 cm^{-1} with a resolution of 4 cm^{-1}.

3.6.4 Field emission scanning electron microscope (SEM/EDS)

The surface area of samples was coated with gold before characterization by SEM/EDS. (JSM-5800LV, Jeol, Ltd.).

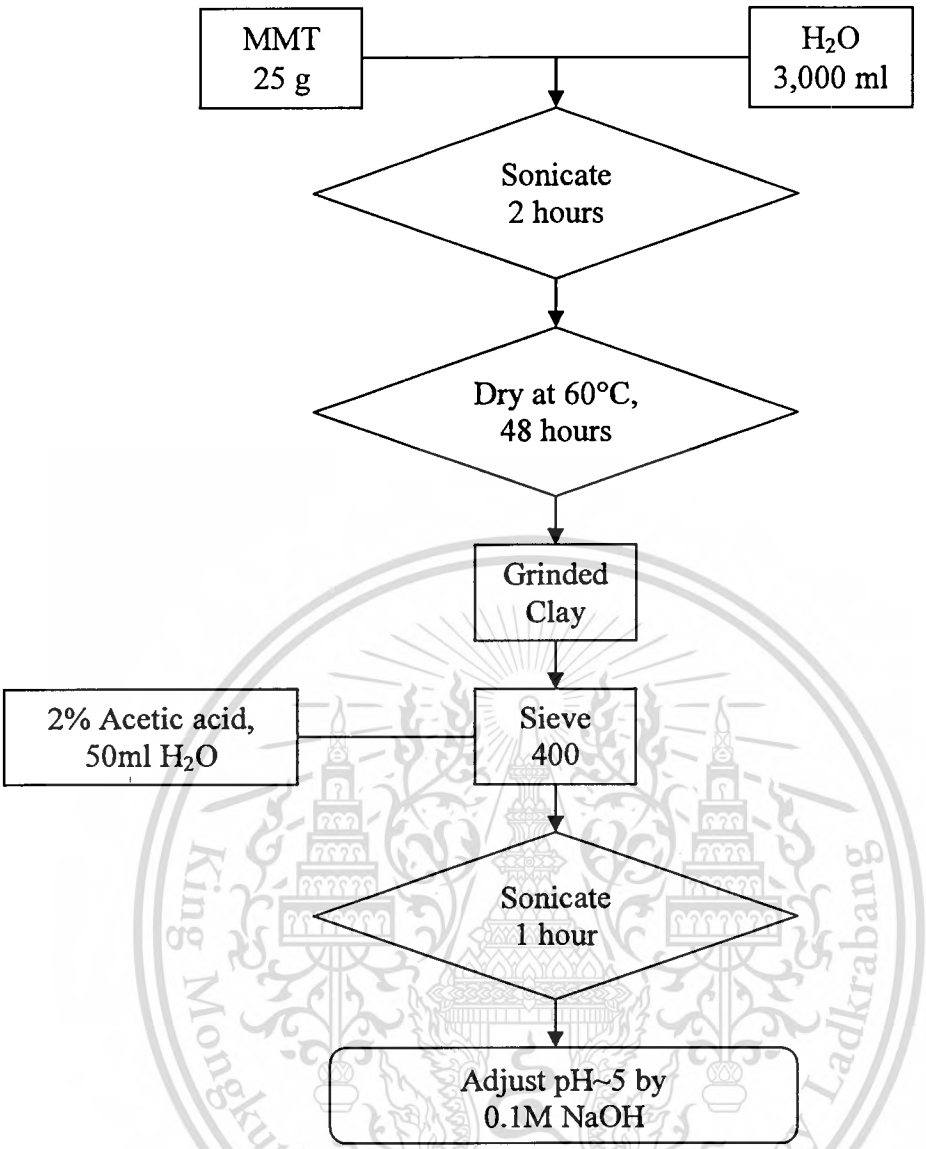

Figure 3.2 Preparation of swelled MMT

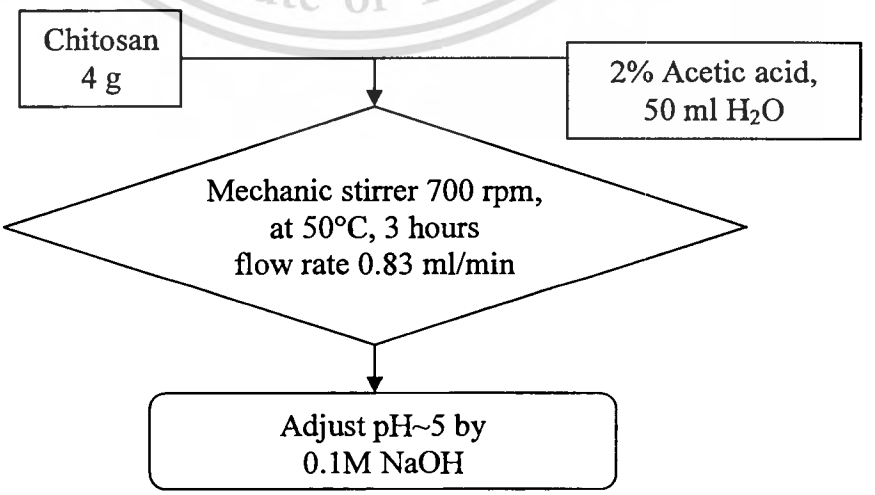

Figure 3.3 Preparation of chitosan solution

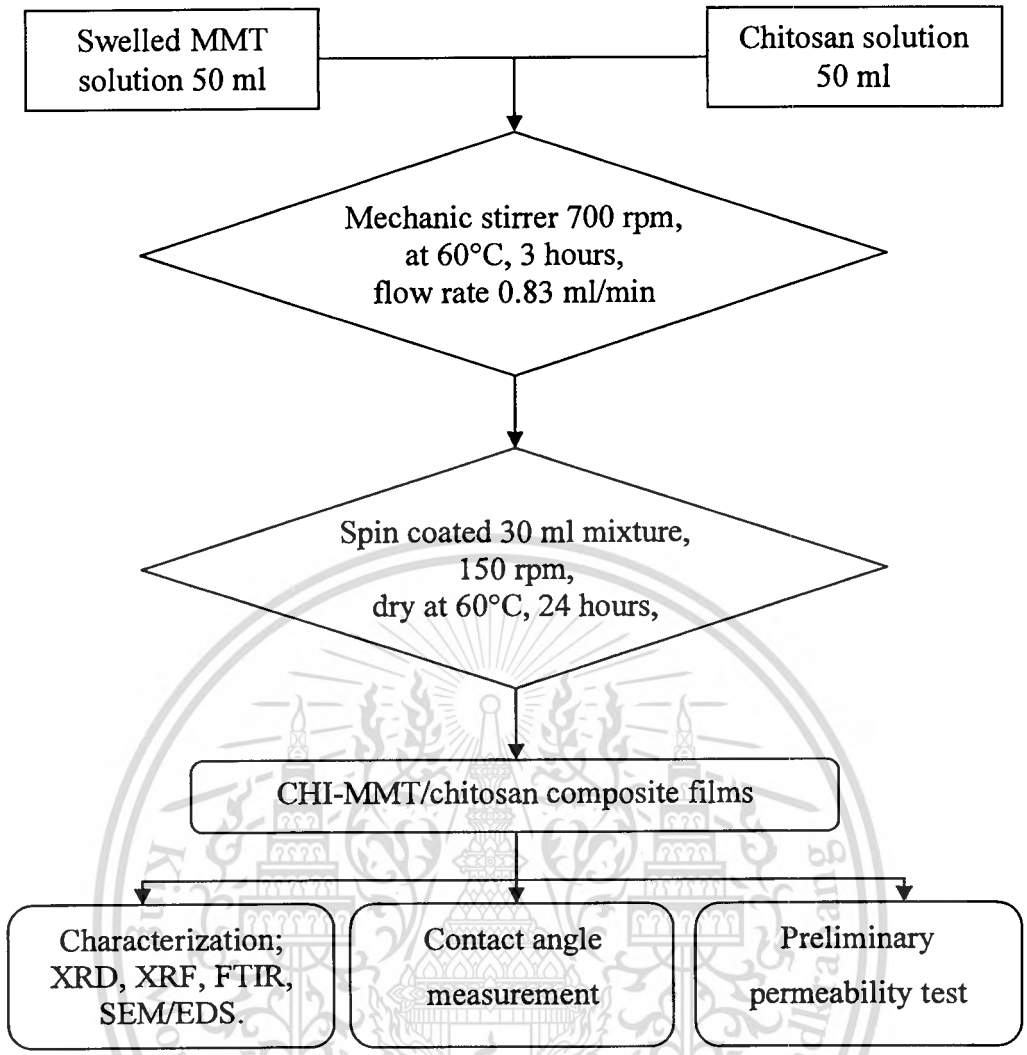

Figure 3.4 Preparation of CHI-MMT/chitosan composite films

Chapter 4

Results and Discussion

The CHI-MMT/chitosan composite films were prepared with various MMT contents, i.e., 1%, 2%, and 3% by weight and coated on filter paper with the order of coating layer and formulae. The films were characterized by XRD, XRF, FTIR, and SEM/EDS. Then, the contact angle measurement and preliminary permeability test were investigated.

4.1 X-ray Diffractometer (XRD)

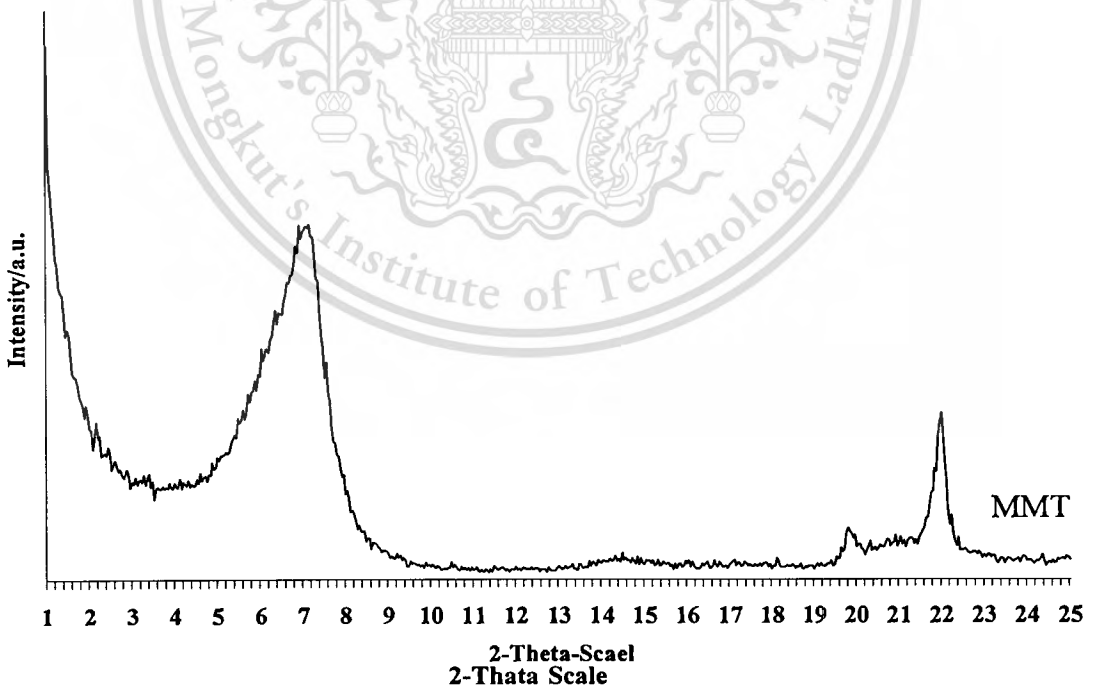

Figure 4.1 XRD pattern of MMT

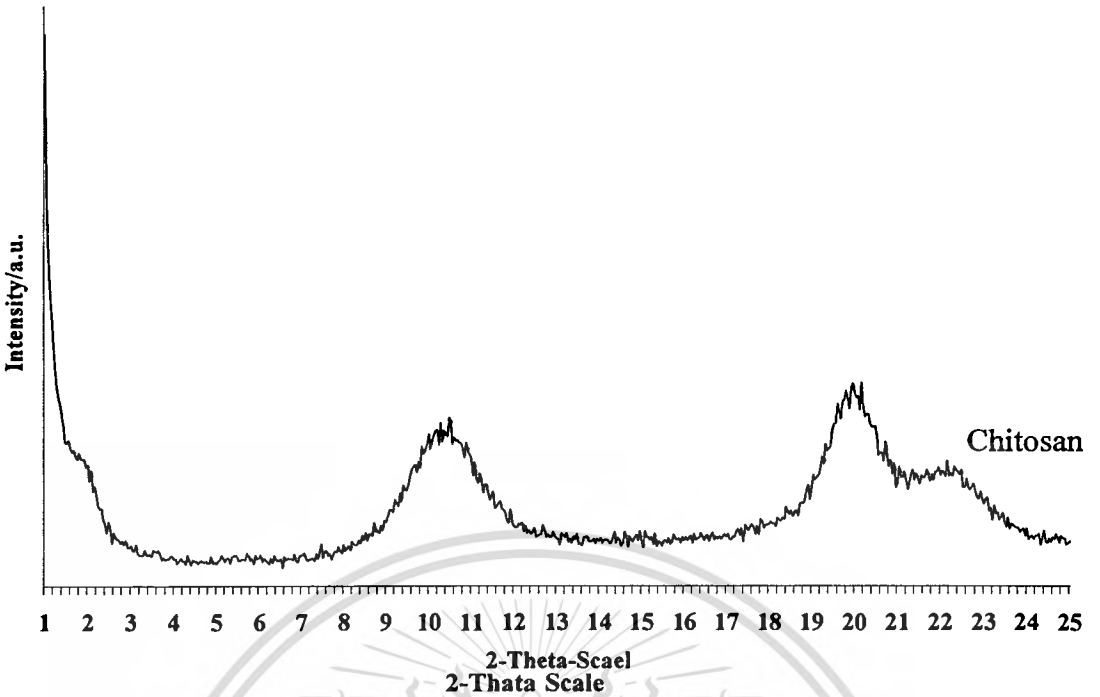

Figure 4.2 XRD pattern of chitosan

Figures 4.1 and 4.2 show the XRD patterns of starting MMT and chitosan. The XRD pattern of MMT showed the crystalline peak at around $2\theta=7.12°$, corresponding to d_{001} of 12.4 Å. The XRD pattern of chitosan was showed broad peaks of chitosan at $2\theta=10.5°$ and 19.8°

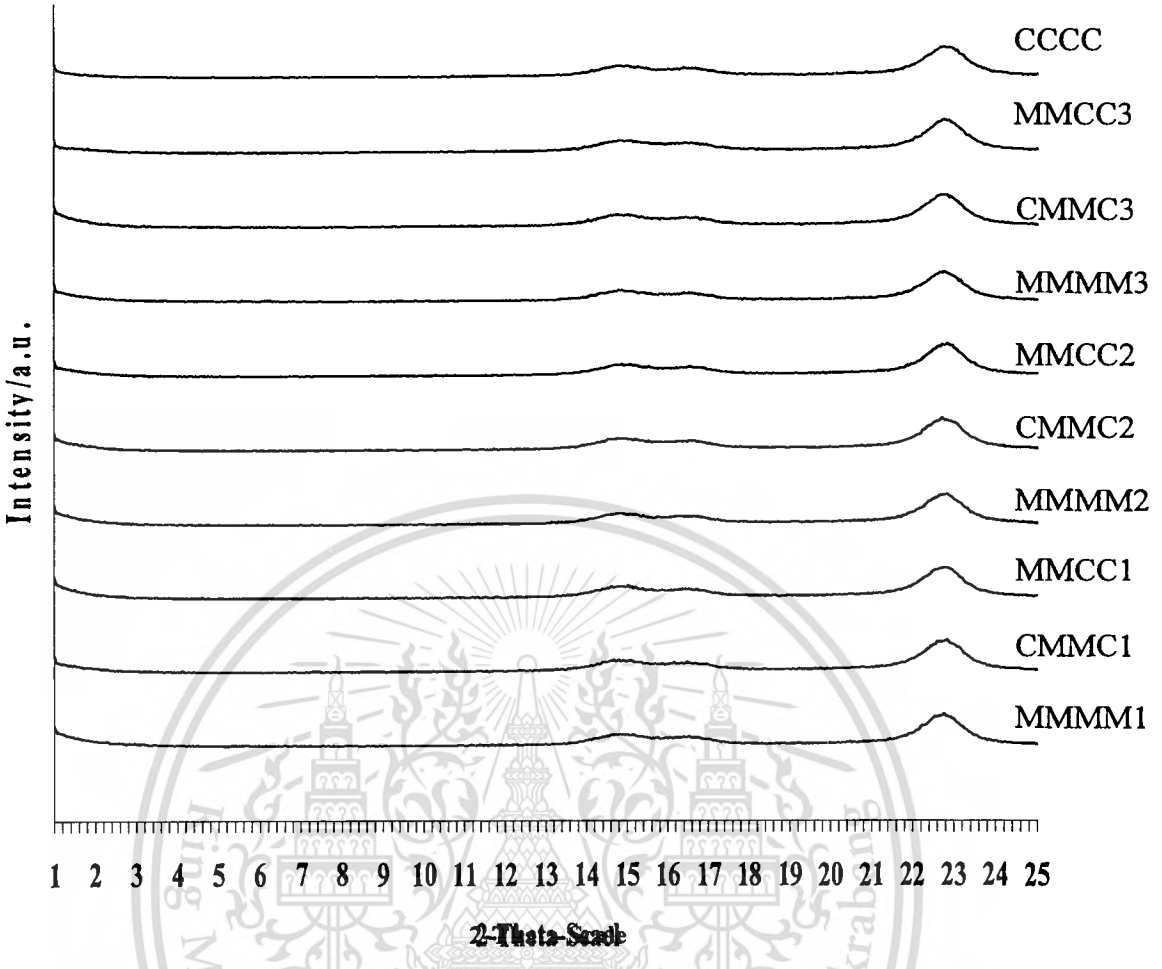

Figure 4.3 XRD patterns of chitosan and CHI-MMT/chitosan composite films

Figure 4.3 shows the XRD patterns of chitosan and CHI-MMT/chitosan composite coated on filter papers. All XRD patterns mainly composed of the crystalline peaks at 2θ=14.8° and 22.7°, corresponding to cellulose from filter paper. The diffraction signals of chitosan and modified-MMT could not be observed. These results were considered to be because of the low contents of chitosan and modified-MMT in all composite samples.

4.2 X-ray Fluorescence Spectrometer (XRFs)

Table 4.1 Chemical composition and Si:Al molar ratio of chitosan and CHI-MMT/chitosan composite coated on filter paper.

Sample	SiO_2 (%)	Al_2O_3 (%)	Na_2O (%)	Other (%)	Si : Al
MMMM1	36.40	6.94	5.13	51.53	0.23
CMMC1	23.80	5.05	4.83	66.32	0.25
MMCC1	6.79	1.58	7.33	84.30	0.28
MMMM2	7.69	1.72	6.48	84.11	0.27
CMMC2	25.30	4.33	5.19	65.18	0.20
MMCC2	35.10	7.08	4.16	53.66	0.24
MMMM3	52.20	10.70	3.36	33.74	0.24
CMMC3	29.20	5.15	-	65.65	0.21
MMCC3	51.10	9.80	3.23	35.87	0.23
CCCC	29.20	4.56	6.94	59.27	0.19

Table 4.1 shows chemical composition and Si:Al molar ratio of chitosan and CHI-MMT/chitosan composite coated on filter paper. It was found that the SiO_2 and Al_2O_3 were detectable in all coated filter papers, indicating the presence of modified-MMT.

4.3 Fourier Transform Infrared Spectrophotometer (FTIR)

Figure 4.4 shows the FTIR spectra of CHI-MMT/chitosan composite films. The peak of the starting MMT gave vibration band as follow; υ_{OH} for –OH stretching with the range at 3630-3620 $cm^{-1}$and υ_{HOH} for H-O-H ~ 1650-1620 cm^{-1}.The major peaks of chitosan at υ_{NH3} for N-H ~ 1600-10 cm^{-1}, and υ_{CO} of C=O ~ 1650-1620 cm^{-1}. The FTIR spectrum of CHI-MMT/chitosan composite films was shown the peak of υ_{HOH} for H-O-H that was overlapped peak between water in starting MMT and COO^- counter ions of chitosan in acetic acid. The peak of υ_{NH3} for N-H ~1600-1650 cm^{-1} was also found in compost indicated that composite had the chitosan component.

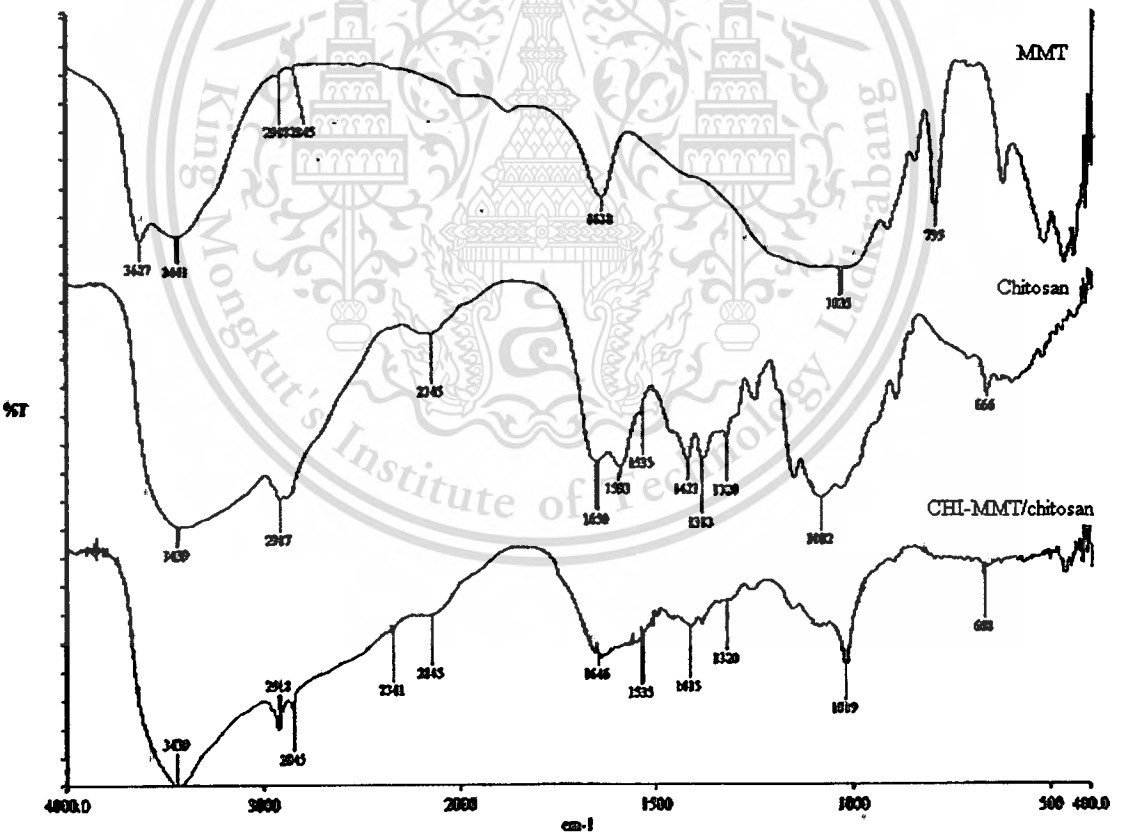

Figure 4.4 Spectra of MMT, chitosan, and CHI-MMT/chitosan composite films (MMCC3)

Table 4.2 Absorption band assignments of the starting MMT, chitosan, and CHI-MMT/chitosan composite coated on filter paper (MMCC3)

Formula no.	Frequencies (cm^{-1})	Assignment
MMT	~3630-3620	-OH stretching
	~1650-1620	H-O-H bonding
	~1050-1040	-Si-O stretching
Chitosan film	~2926-2915	-CH stretching
	~1650-1620	-C=O stretching
	~1600-1560	-NH bending
MMT-Chitosan	~3630-3620	-OH stretching
	~2926-2915	-CH stretching
	~1640-1635	-C=O stretching (overlapped) H-O-H bending (overlapped)
	~1600-1650	-NH bending

4.4 Field Emission Scanning Electron Microscope (FESEM/EDS)

Figure 4.5 shows SEM micrographs and silicon mapping of chitosan and CHI-MMT/chitosan composite coated on filter papers. From the SEM micrographs, all samples showed the continuous phase of chitosan impregnated in the space among the cellulose fibrous. It was, however, the particles containing silicon might be observed in some particular areas of CHI-MMT/chitosan composite coated filter papers. These particles were assumed to be either unmodified MMT or chitosan modified MMT.

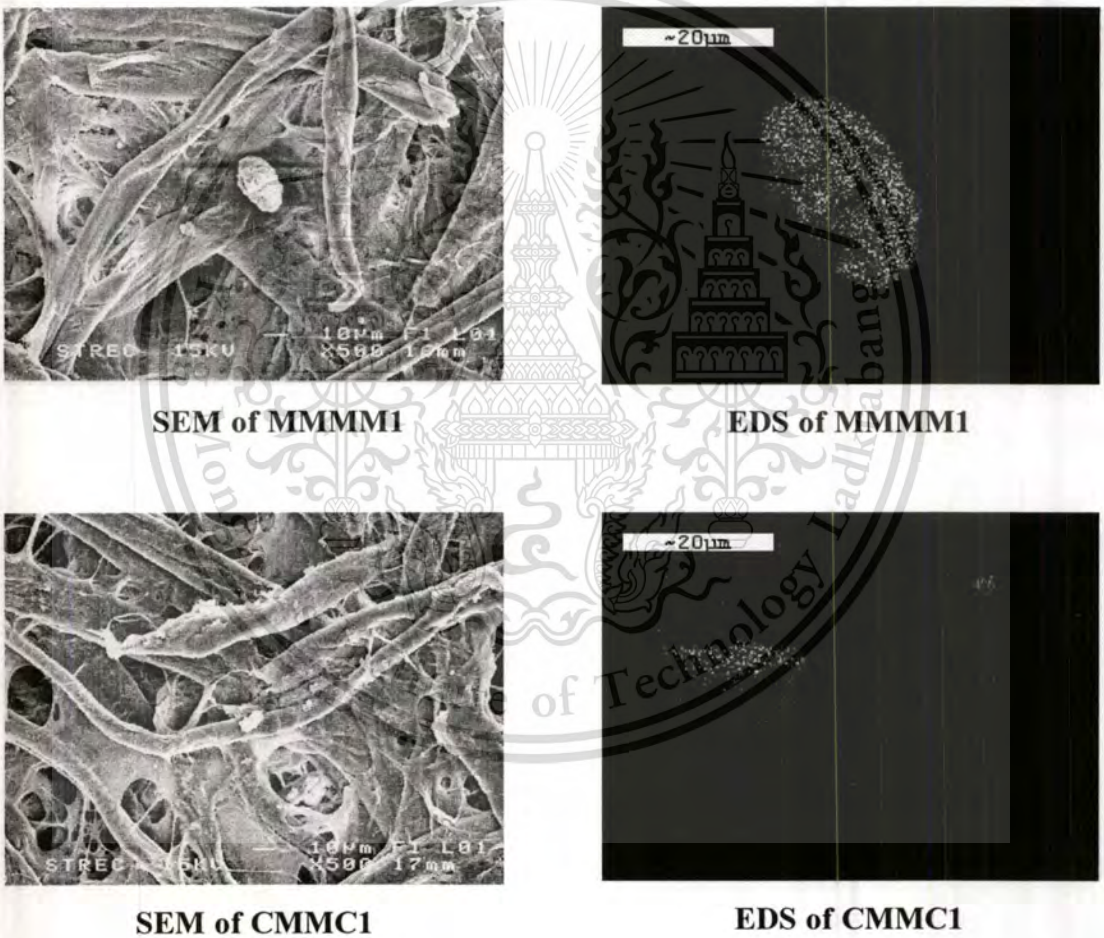

SEM of MMMM1 EDS of MMMM1

SEM of CMMC1 EDS of CMMC1

Figure 4.5 SEM micrographs and silicon mapping of chitosan and CHI-MMT/chitosan composite coated on filter papers.

SEM of MMCC1

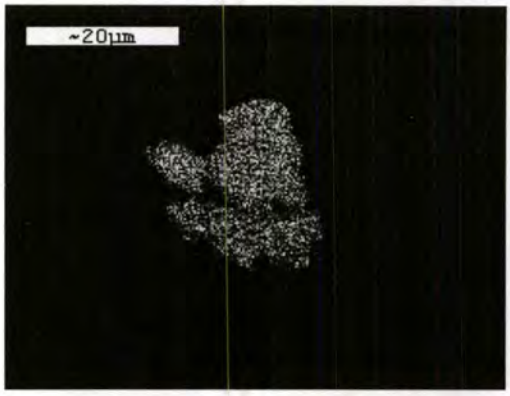

EDS of MMCC1

SEM of MMMM2

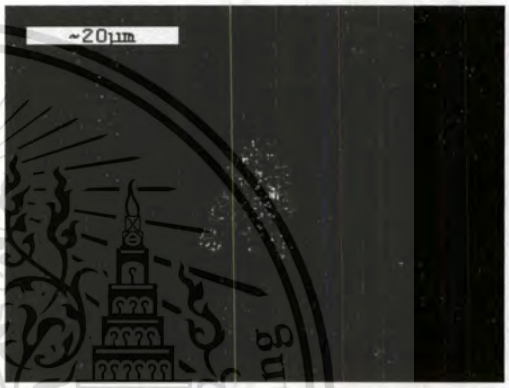

EDS of MMMM2

SEM of CMMC2

EDS of CMMC2

Figure 4.5 (Continued)

SEM of MMCC2

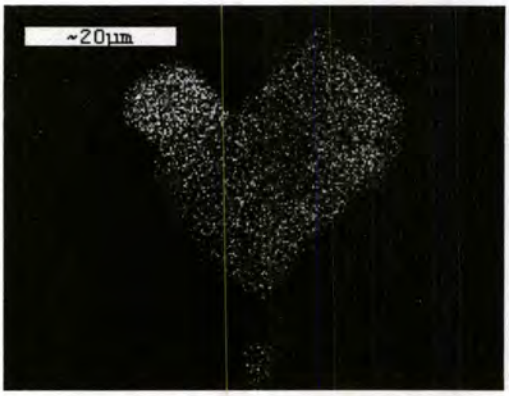

EDS of MMCC2

SEM of MMMM3

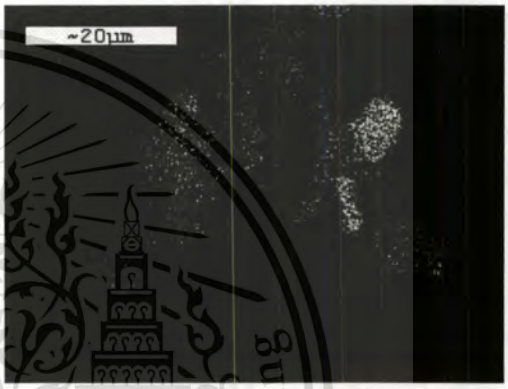

EDS of MMMM3

SEM of CMMC3

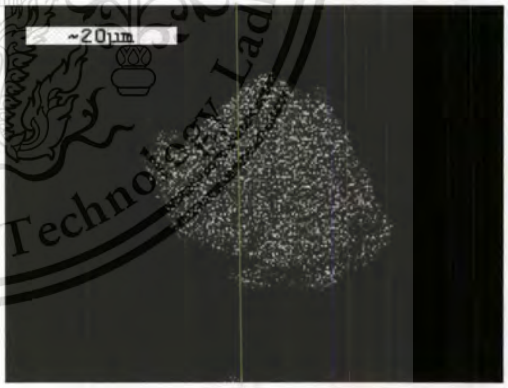

EDS of CMMC3

Figure 4.5 (Continued)

SEM of MMCC3

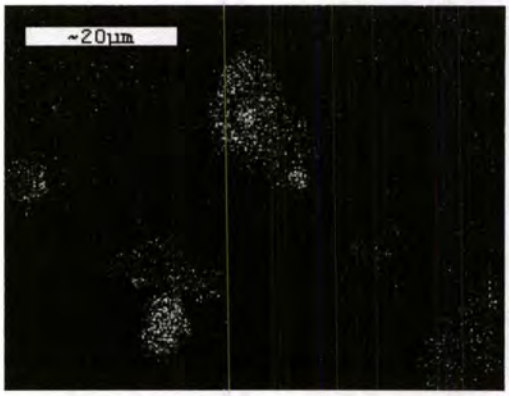

EDS of MMCC3

SEM of CCCC 3

EDS of CCCC3

Figure 4.5 (Continued)

4.5 Contact Angle Measurement

The chitosan coated on filter paper (CCCC) showed the highest initial contact angle of 115° due to its low polarity in comparison with water. When measurement time increased, the contact angle would decrease due to the penetration of water into filter paper. The presence of MMT in the CHI-MMT/chitosan composite caused decreasing in contact angle of the coated papers. This result was because the polarity of MMT is similar to water, resulting in higher wettability.

In case of four layers of CHI-MMT/chitosan composite coated on filter papers (MMMM), the initial contact angle decreased with an increase of MMT content, indicating the higher wettability. The $\Delta\theta$ values between the CCCC and MMMM samples, the CCCC showed higher $\Delta\theta$ than MMMM samples. These results indicated that the CCCC allowed higher water penetration than MMMM samples. This result was because the crystalline structure of MMT impeded the water penetration.

In case of MMCC samples, the lowest contact angle was obtained due to good wettability. Moreover, the highest $\Delta\theta$ value was also obtained because better swelling of chitosan inner layers promoted the water permeability.

These results were attributed to the presence of MMT in the second and third inner layer, resulting in the higher wettability than MMCC samples. It was, however, the $\Delta\theta$ of CMMC was lower than that of MMCC because the penetration of water through the 2^{nd} and 3^{rd} MMT inner layers was diminished.

Table 4.3 Contact angle of CHI-MMT/chitosan coated on filter papers

Formula	Contact Angle (degree)			Δθ	
	0 sec	30 sec	60 sec	Δ 0-30 sec	Δ 0-60 sec
MMMM1	99.9	95.9	93.8		
	99.7	98.3	N/A		
Average	99.8	97.1	93.8	2.7	6.0
CMMC1	97.4	90.9	82.8		
	95.9	91.7	88.9		
Average	96.7	91.3	85.9	5.4	10.8
MMCC1	86.3	68.2	N/A		
	87.9	75.7	48.4		
Average	87.1	71.95	48.4	15.2	38.7
MMMM2	88.6	82.2	75.8		
	95.6	91.8	85.0		
Average	92.1	87.0	80.4	5.1	11.7
CMMC2	95.6	91.8	89.5		
	94.8	92.9	91.2		
Average	95.2	92.4	90.4	2.9	4.9
MMCC2	82.3	67.3	58.9		
	82.1	68.2	N/A		
	81.5	63.6	49.6		
Average	82.0	66.4	54.3	15.6	27.7
MMMM3	92.0	90.3	87.2		
	92.7	89.3	88.4		
	92.0	89.7	85.5		
Average	92.2	89.8	87.0	2.5	5.2
CMMC3	92.5	86.2	81.4		
	93.1	88.4	84.2		
Average	92.8	87.3	82.8	5.5	10.0
MMCC3	94.2	72.0	58.0		
	95.9	77.9	63.4		
	93.0	60.7	57.4		
Average	94.4	70.2	59.6	24.2	34.8
CCCC	114.1	102.1	98.9		
	116.8	109.0	86.6		
Average	115.5	105.6	92.8	9.9	22.7

4.6 Preliminary Permeability Test

Figure 4.6 shows the change of percentage of moisture content/g of anhydrous Na_2SO_4 with time. The chitosan and CHI-MMT/Chitosan composite coated on filter papers showed lower moisture content and lower rate of weight change (slope=0.0159-0.0976 percentage of moisture/g-Anhydrous Na_2SO_4 per day) than the uncoated filter paper (slope=0.1038 percentage of moisture/g-Anhydrous Na_2SO_4 per day), indicating the increasing of moisture penetration through the coated filter papers. This result was because the porous of filter paper was blocked with the coated substances.

The CCCC showed higher weight change than MMMM samples. These results indicated that the CCCC allowed higher moisture penetration than MMMM samples because the crystalline structure of MMT impeded the moisture penetration.

The CMMC samples showed higher permeability than the MMMM samples, but lower than the MMCC samples. The MMCC samples showed the highest permeability because of good wettability of outer MMT layer as discussed previously (section 4.5). The permeability exhibited the same trend as the rate of contact angle change. These results indicated that the alternative moisture permeability could be achieved by differ coated sequence.

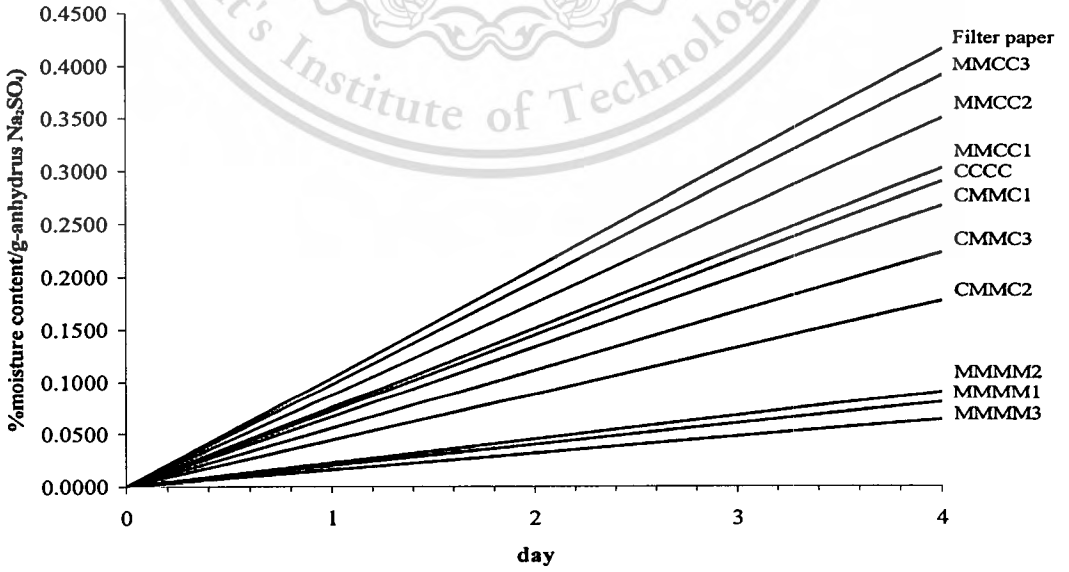

Figure 4.6 Percentage of moisture content per gram of anhydrous Na_2SO_4 (filter paper) and (CHI-MMT/chitosan composite coated on filter papers)

Chapter 5

Conclusion and Suggestion

5.1 Conclusion

The CHI-MMT/chitosan solutions were prepared using various MMT contents, i.e. 1%, 2% and 3% weights. The sequence of coated layer on filter papers had the effects on water wettability and penetration rate. CCCC allowed higher water and moisture penetration than MMMM samples according to higher $\Delta\theta$ values and weigh change. In case of MMCC samples, the lowest contact angle was obtained due to good wettability and better swelling of chitosan inner layers promoted the water and/or moisture permeability.

5.2 Suggestion for Future Works

1. The composite films should be prepared without filter paper or with other substrates e.g. nylon meshes.
2. Preparation of the CHI-MMT/chitosan composite films for controllable permeability of water and moisture.
3. More study on permeability test should be carried out.

References

[1] http://crazyblogspot.com/2007/09

[2] http://en.wikipedia.org/wiki/clay

[3] http://mineral.galleries.com/minerals/silicate/clays.htm

[4] http://www.amazon.com/details.asp?ArticleiD=96

[5] http://encyclopedia.thefreedictionary.com/Montmorillonite

[6] http://dalwoo.com/chitosan/21c.htm

[7] http://encyclopedia.thefreedictionary.com/chitosan

[8] http://callisto.si.usherb.ca/~rbrzezin/what_is_chitosan.htm

[9] http://www.vanderbilt.edu/AnS/psychology/health_ psychology/chitosanl.htm

[10] http://dalwoo.com/chitosan/whatischitosan.html#top

[11] http://dalwoo.com/chitosan/preparation.html

[12] http://dalwoo.com/chitosan/chito9htm

[13] http://salwoo.com/chitosan/funtional.htm

[14] William Gacitua E., Aldo Ballerini, Jinwen Zhan, 2003, **Polymer Nanocomposites: Synthetic and Natural Fillers Review**.

[15] Darder M, Collila M, and Ruiz-Hitzky E, 2003, "Chitosan–clay nanocomposites: application as electrochemical sensors" **Applied Clay Science.** Issues 1-4, January 2005, Pages 199-208.

[16] Adriana Czimerova, L'ubos Jankovic, and Jaraj Bujdak, 2004, "Effect of the exchangeable cations on the spectral properties of methylene blue in clay dispersions" **Journal of Colloid and Interface Science** Volume 274, Issue 1, 1 June 2004, Pages 126-132.

[17] Darder M, Lopez-Blanco M, Aranda P, Leroux F, and Ruiz-hitzky E, 2005. "Relevance of polymer– and biopolymer–clay nanocomposites in electrochemical and electroanalytical applications" **Thin Solid Films**. Volume 495, Issues 1-2, 20 January 2006, Pages 104-112.

[18] Darder M, Colilla M, and Ruiz-hitzky E, 2005. "Effect of the exchangeable cations on the spectral properties of methylene blue in clay dispersions" **Journal of Colloid and Interface Science**. Volume 274, Issue 1, 1 June 2004, Pages 126-132

[19] Li Wang, Aiqin Wang, 2007, "Adsorption behaviors of Congo red on the N,O-carboxymethyl-chitosan/montmorillonite nanocomposite" **Chemical Engineering Journal.** Volume 147, Issue 3, 25 August 2007, Pages 979-985.

[20] Kun-Ho Liu, Ting-Yu Liu, San-Yuan Chen, Dean-Mo Liu, 2008, "Drug release behavior of chitosan–montmorillonite nanocomposite hydrogels following electrostimulation" **Acta Biomaterialia**. Available online 8 February 2008.

APPENDIX-A

XRD Patterns of Chitosan and CHI-MMT/Chitosan Composite Coated on Filter Papers

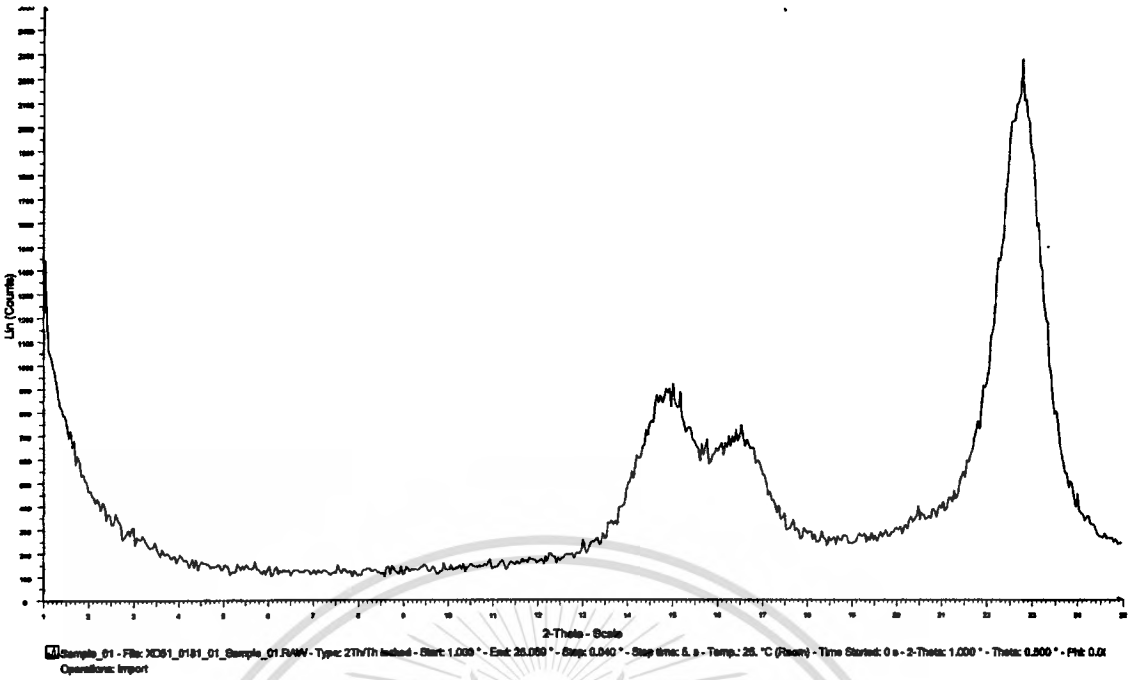

Figure A-1 XRD pattern of MMMM1

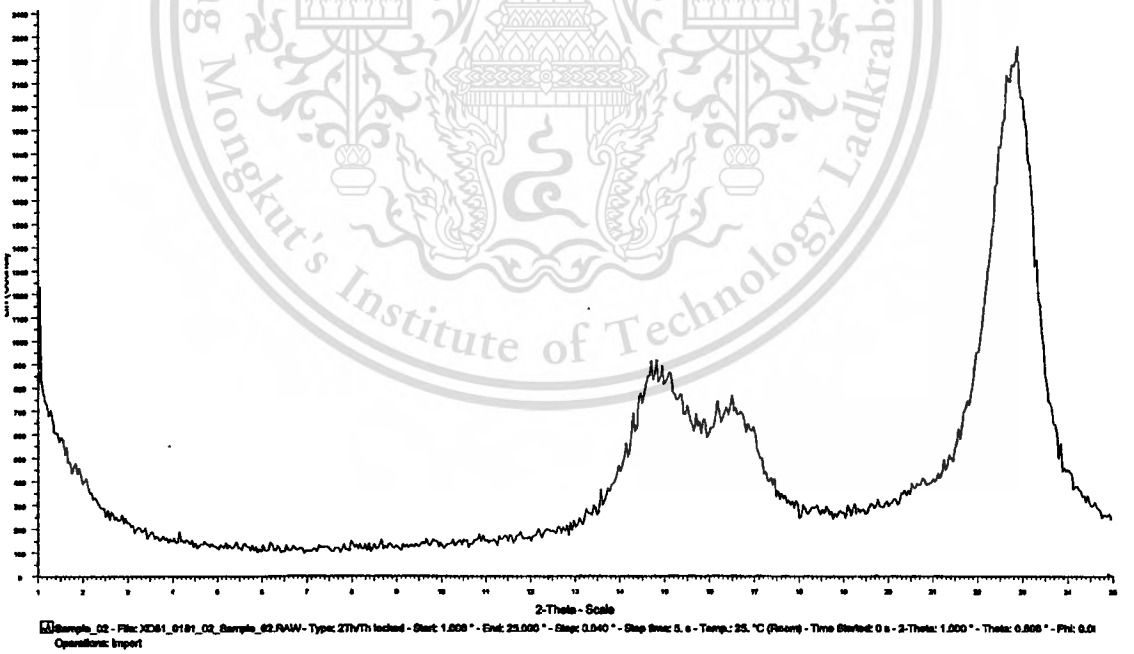

Figure A-2 XRD pattern of CMMC1

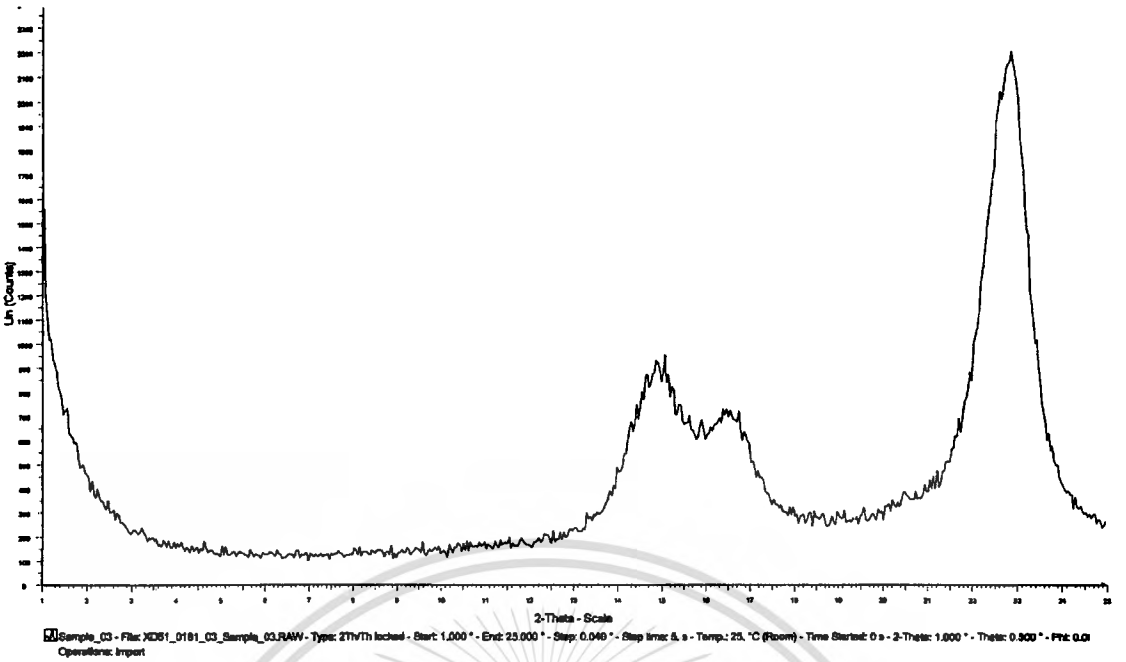

Figure A-3 XRD pattern of MMCC1

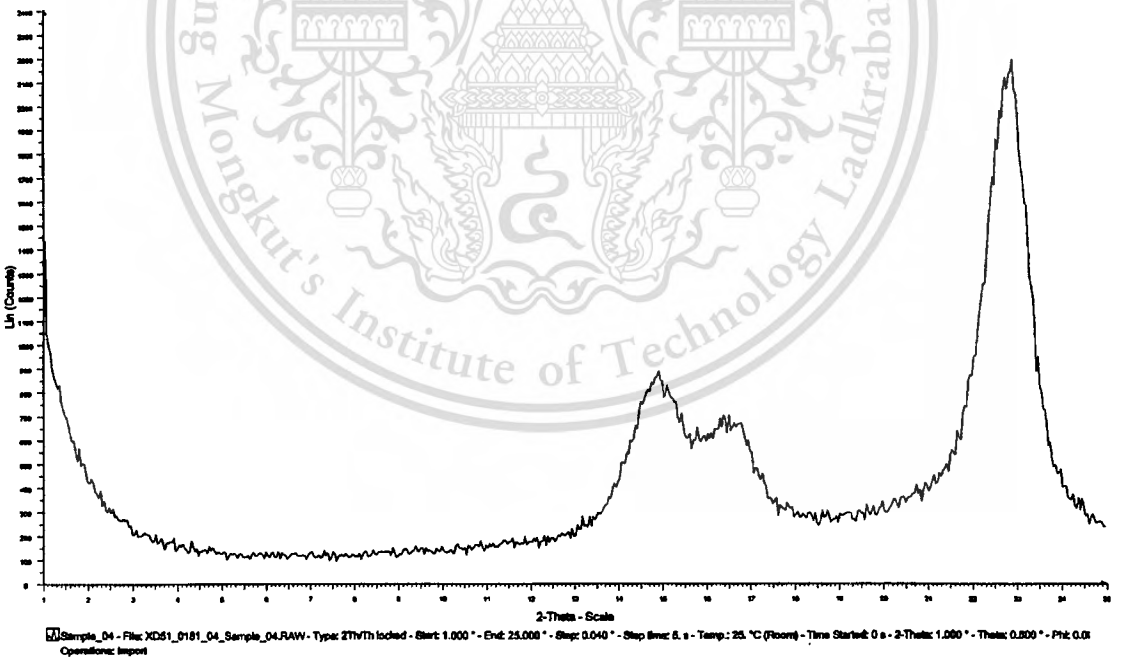

Figure A-4 XRD pattern of MMMM2

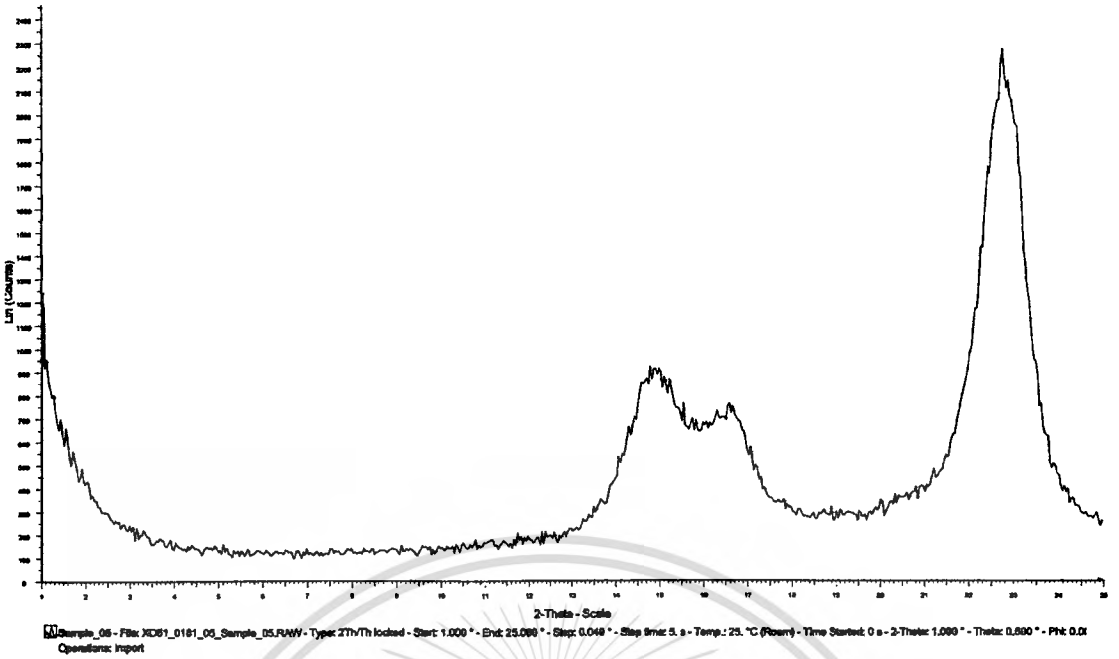

Figure A-5 XRD pattern of CMMC2

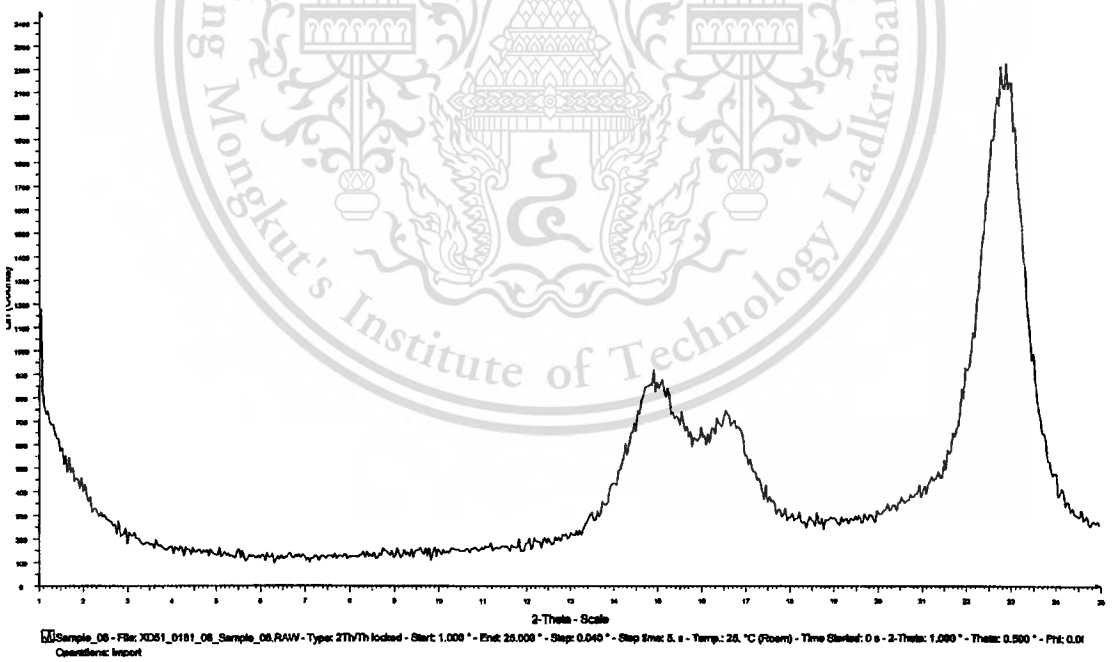

Figure A-6 XRD pattern of MMCC2

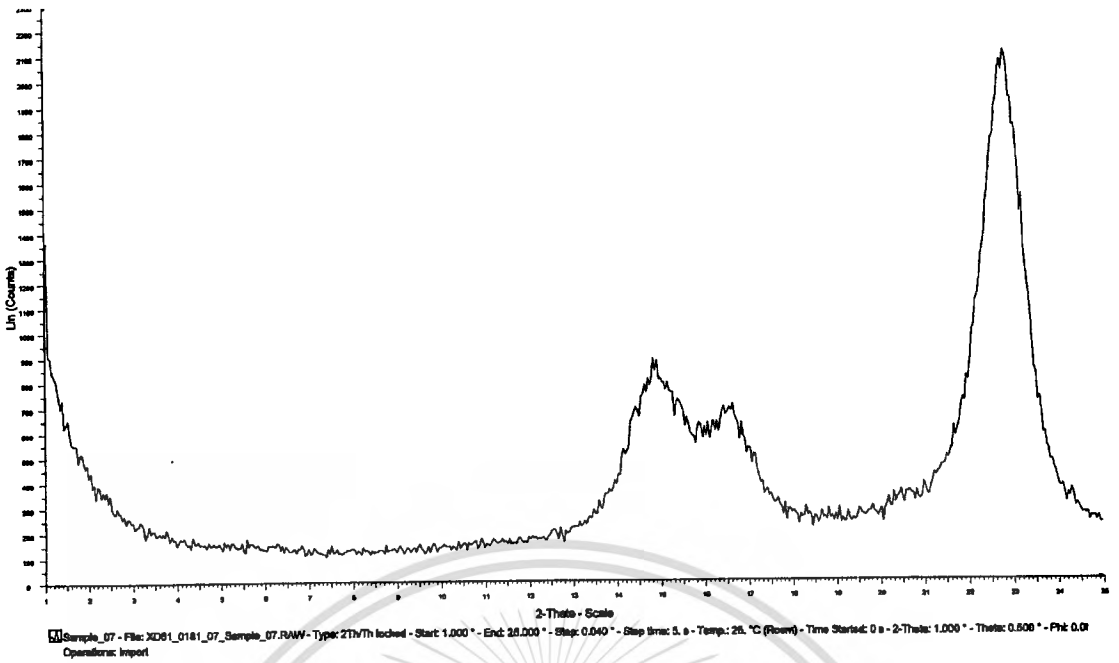

Figure A-7 XRD pattern of MMMM3

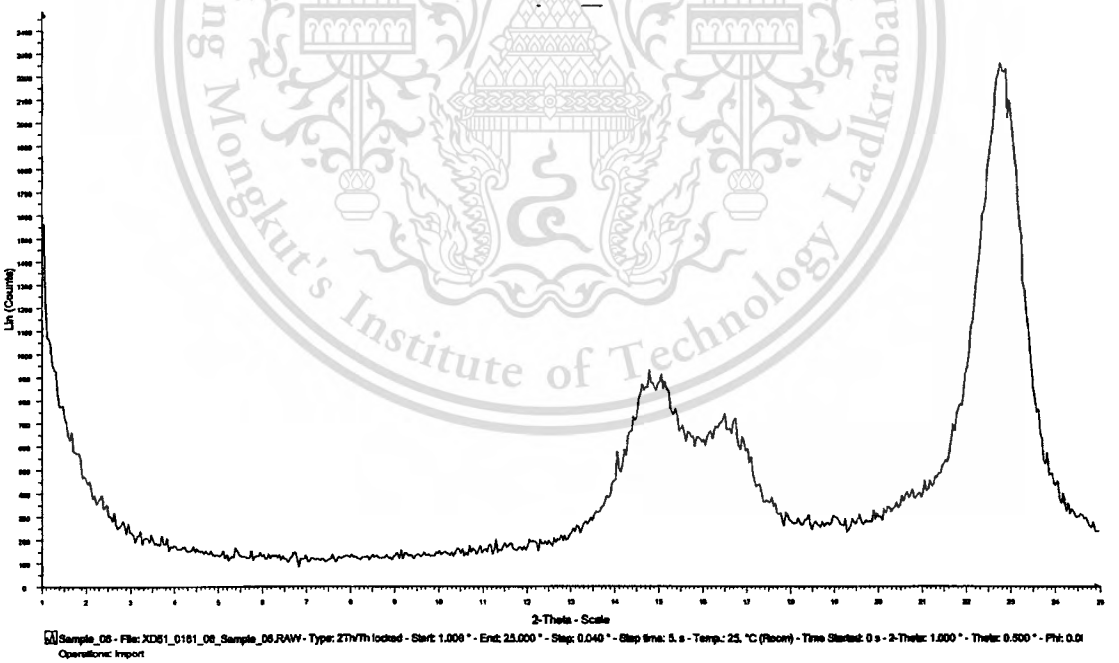

Figure A-8 XRD pattern of CMMC3

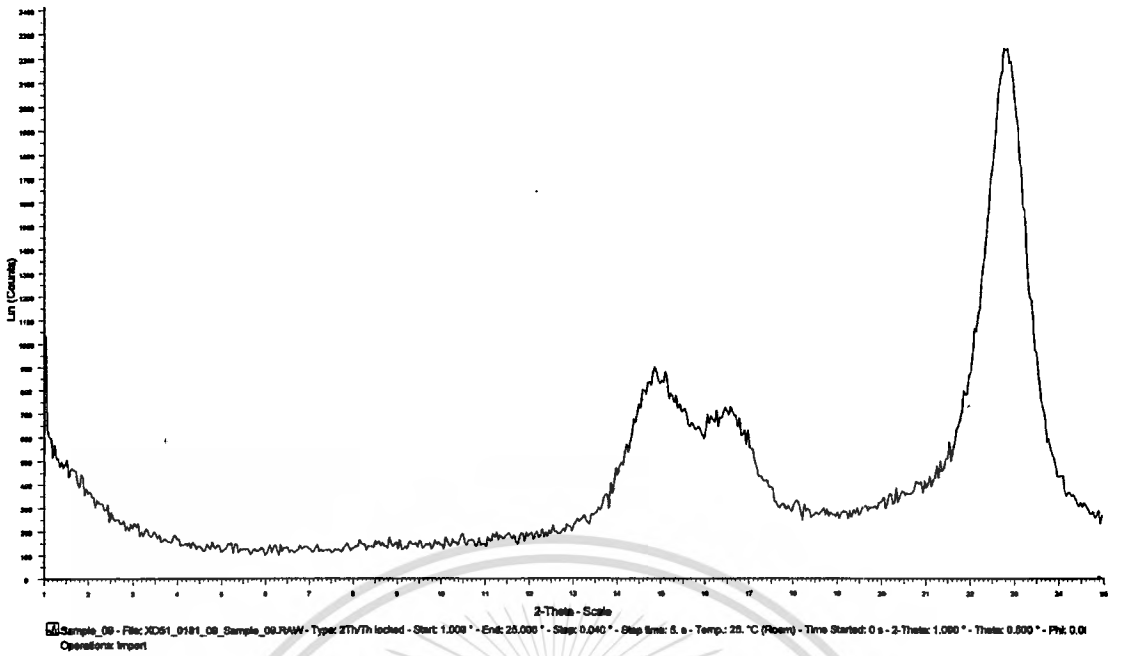

Figure A-9 XRD pattern of MMCC3

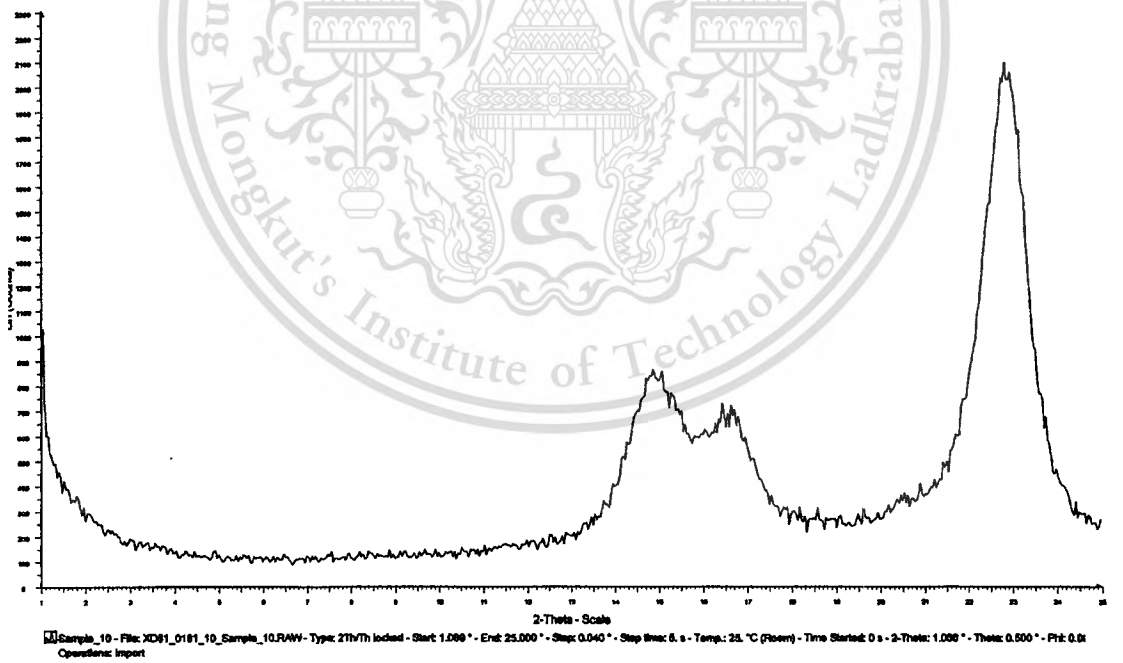

Figure A-10 XRD pattern of CCCC

APPENDIX-B

Spectra of Starting MMT, Starting Chitosan, and CHIMMT/Chitosan Composite Coated on Filter Papers

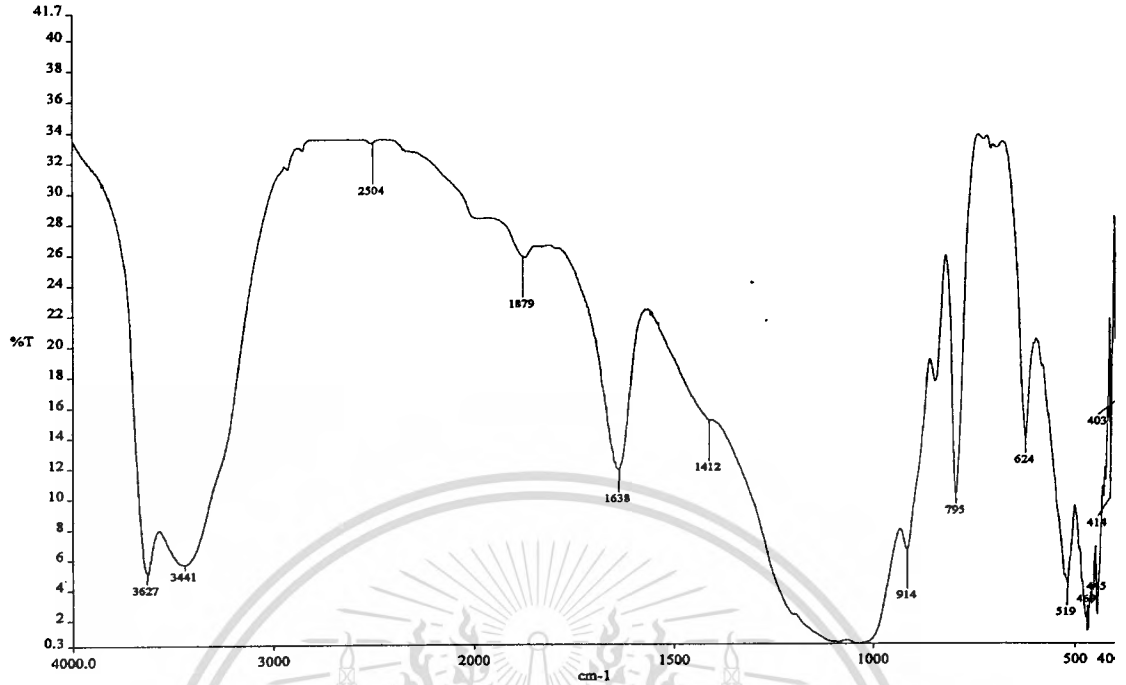

Figure B-1 FTIR spectrum of MMT

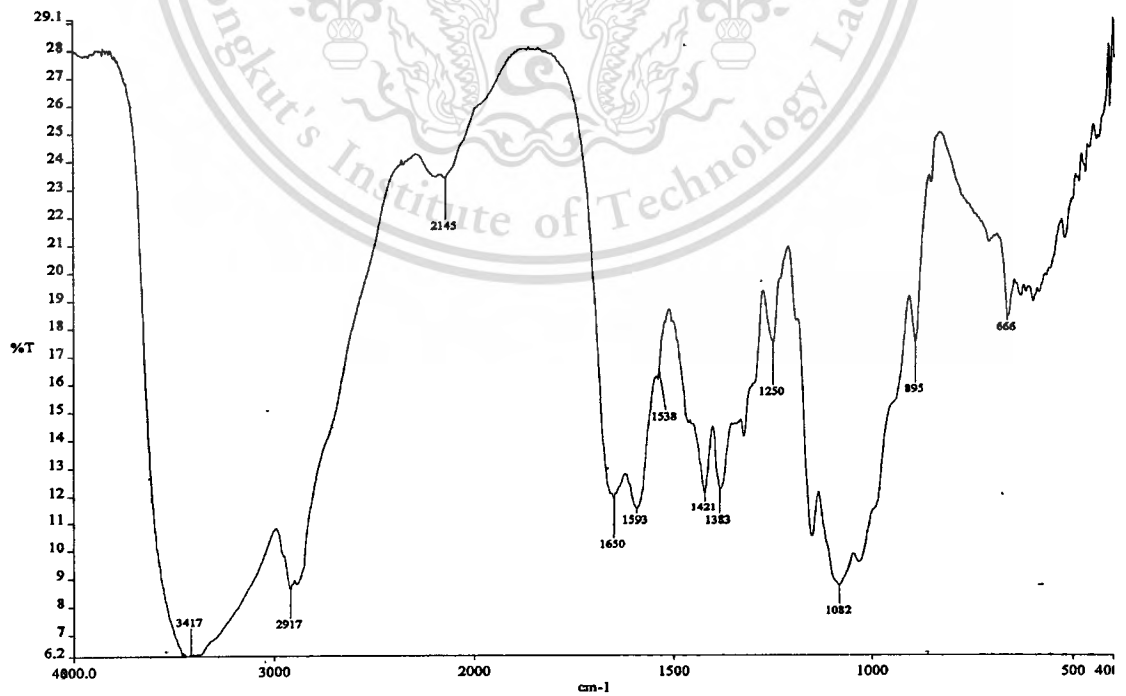

Figure B-2 FTIR spectrum of chitosan

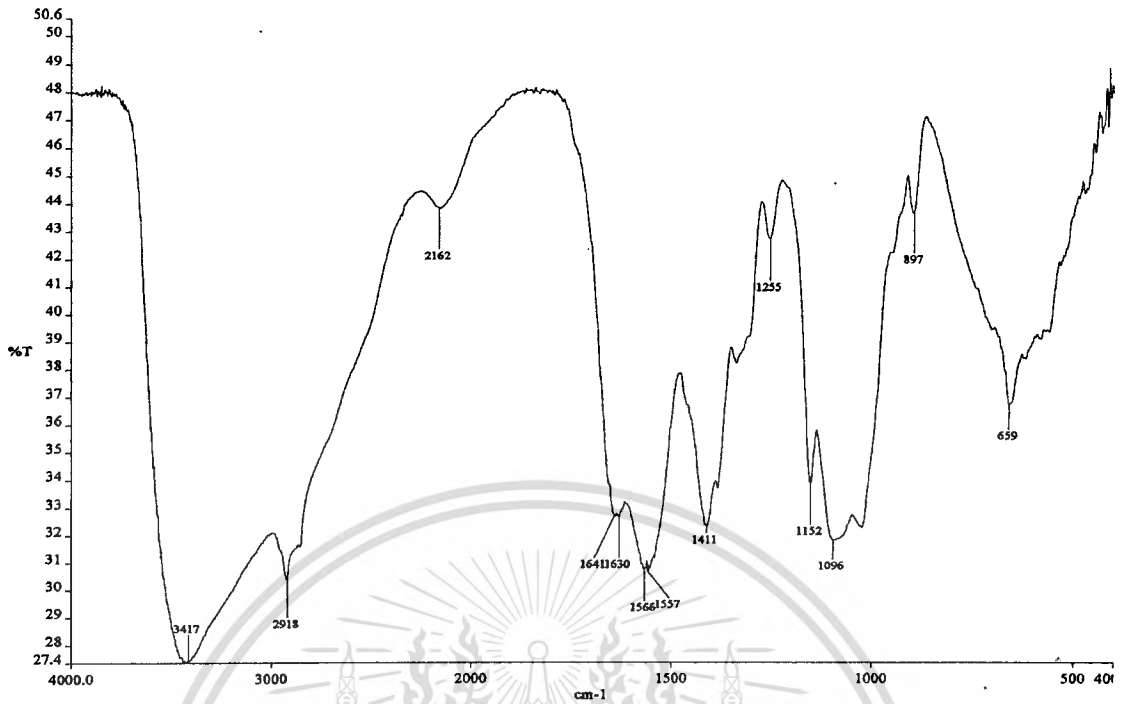

Figure B-3 FTIR spectrum of MMMM1

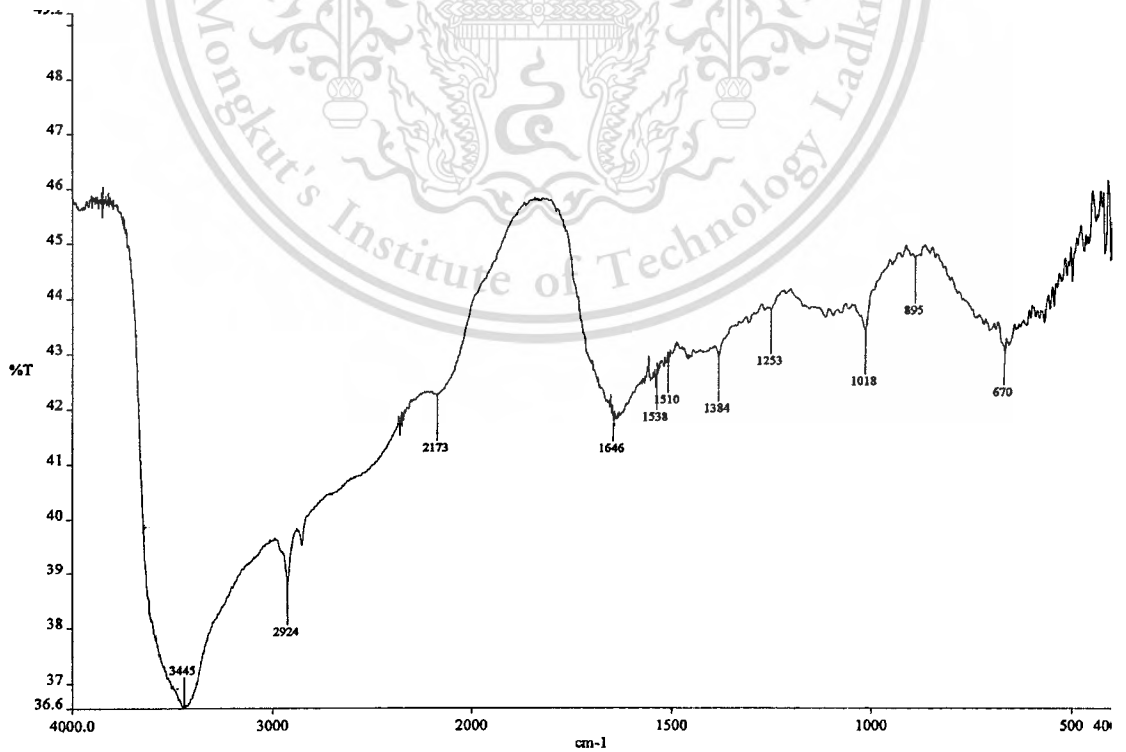

Figure B-4 FTIR spectrum of CMMC1

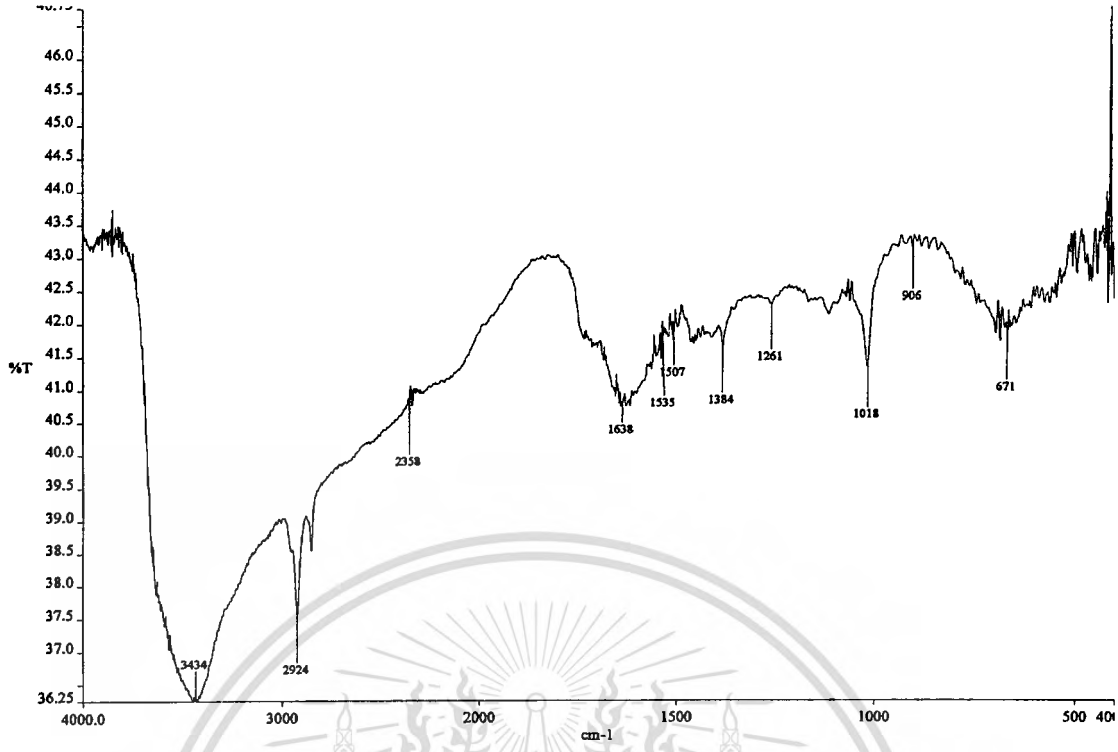

Figure B-5 FTIR spectrum of MMCC1

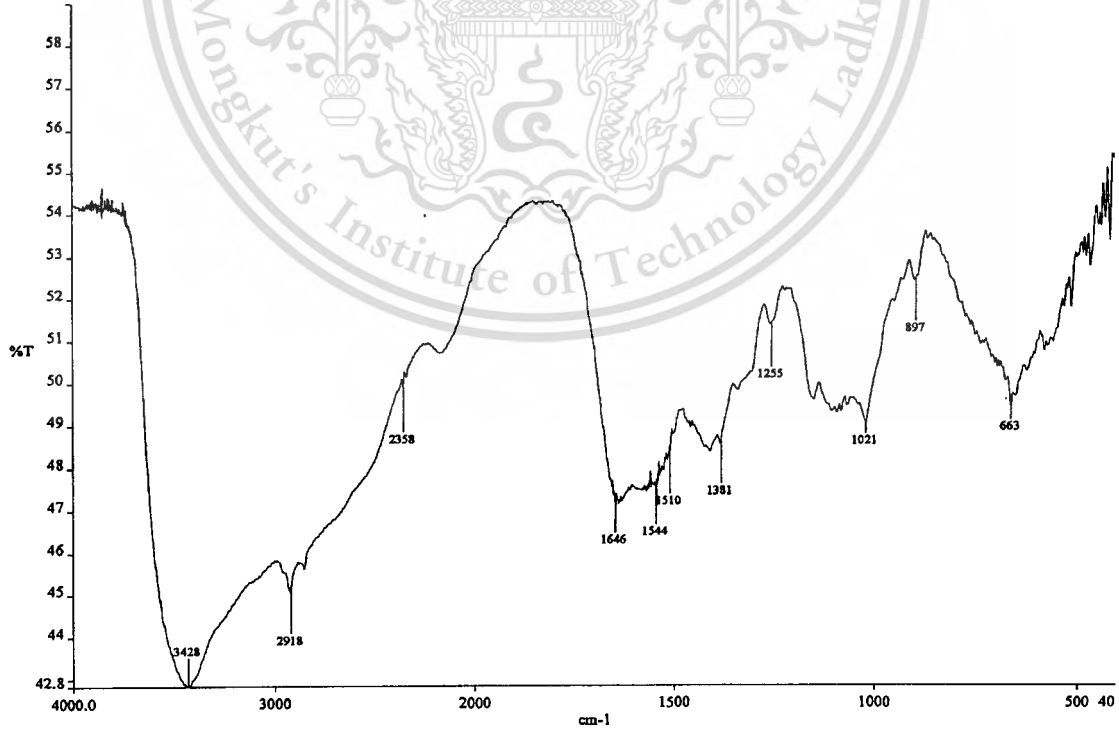

Figure B-6 FTIR spectrum of MMMM2

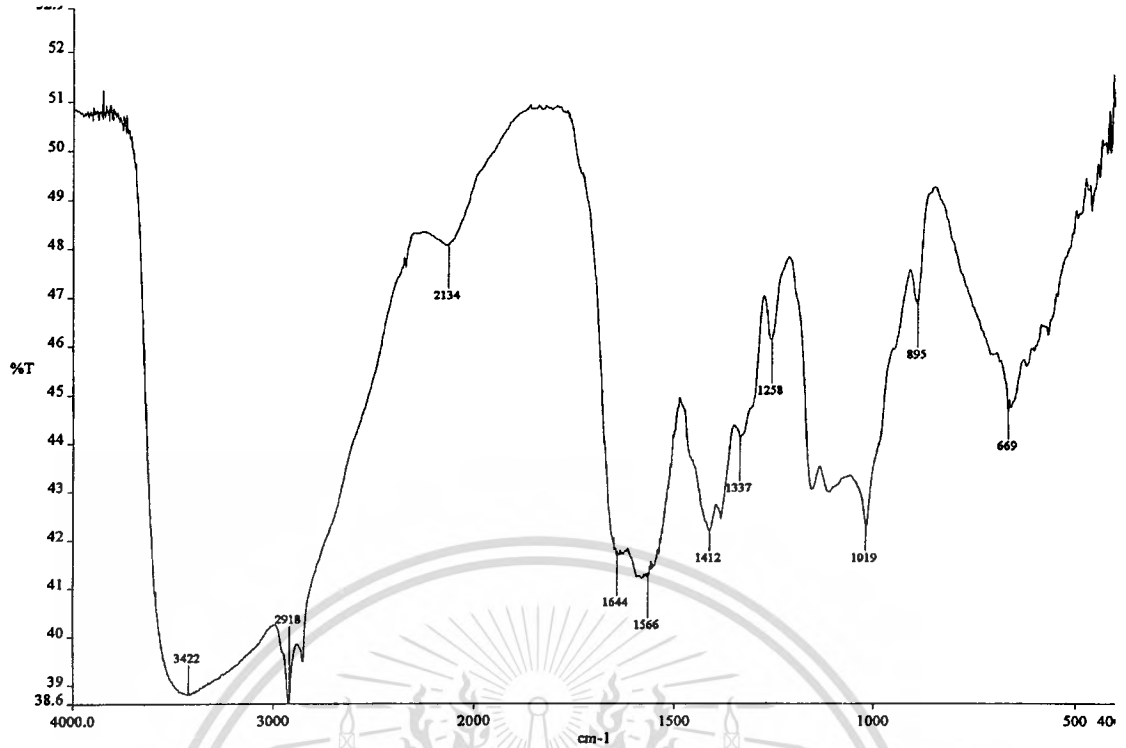

Figure B-7 FTIR spectrum of CMMC2

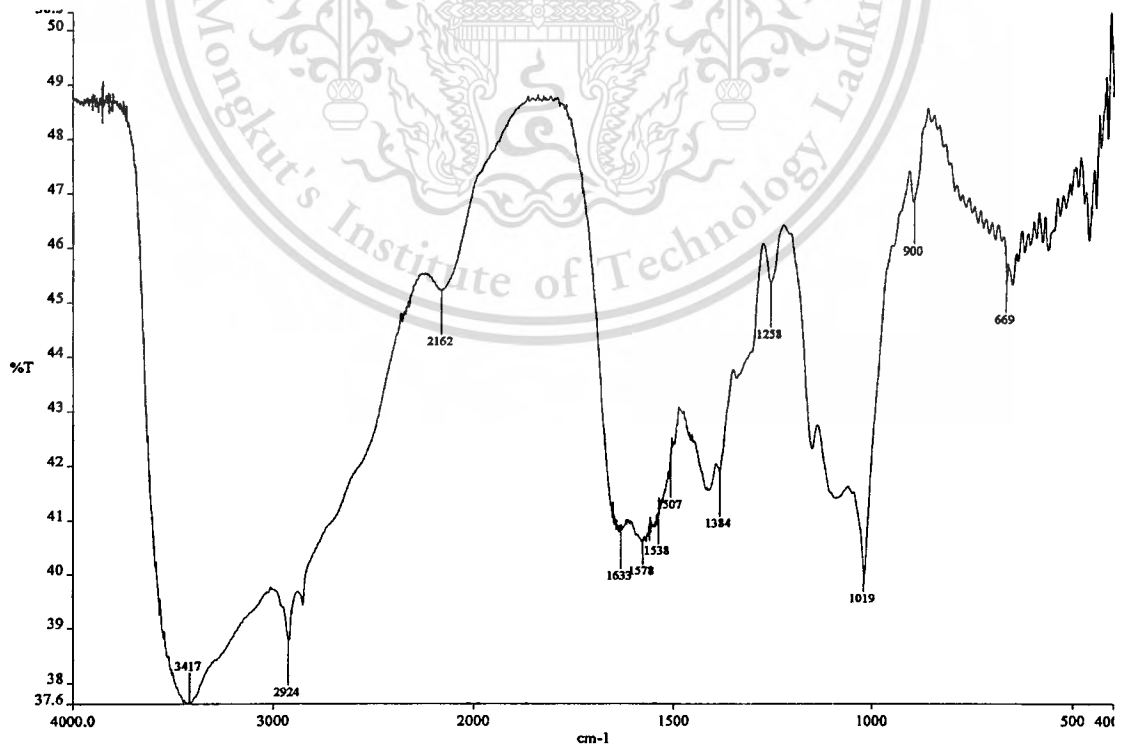

Figure B-8 FTIR spectrum of MMCC2

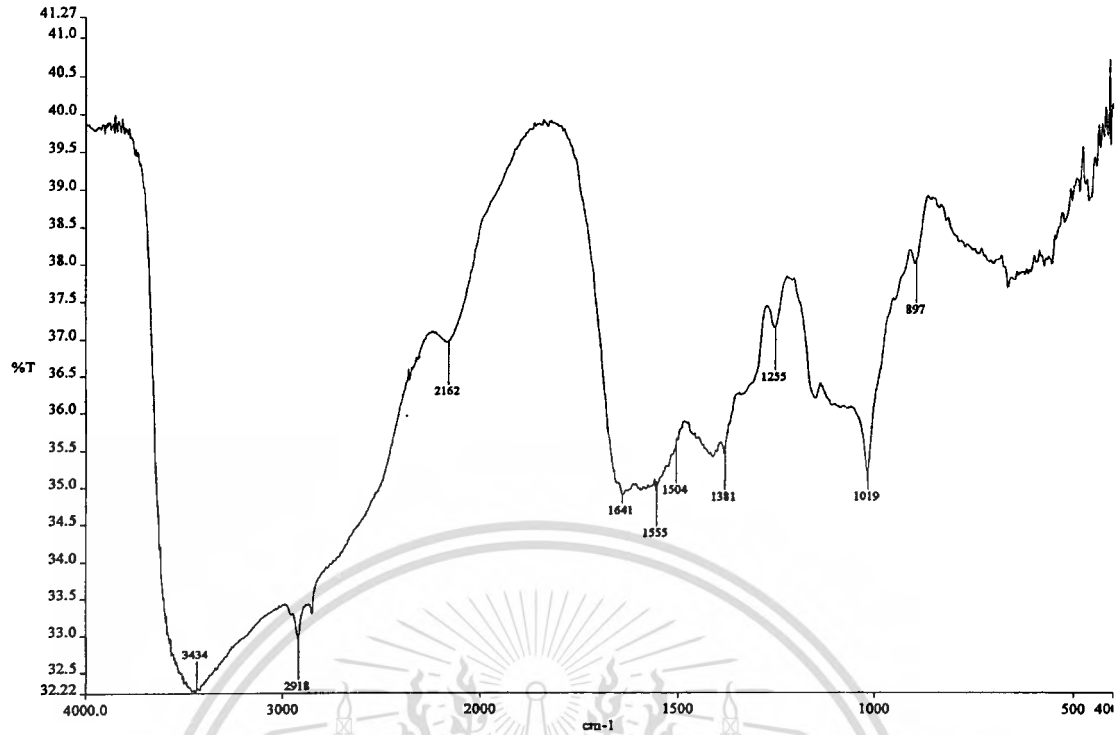

Figure B-9 FTIR spectrum of MMMM3

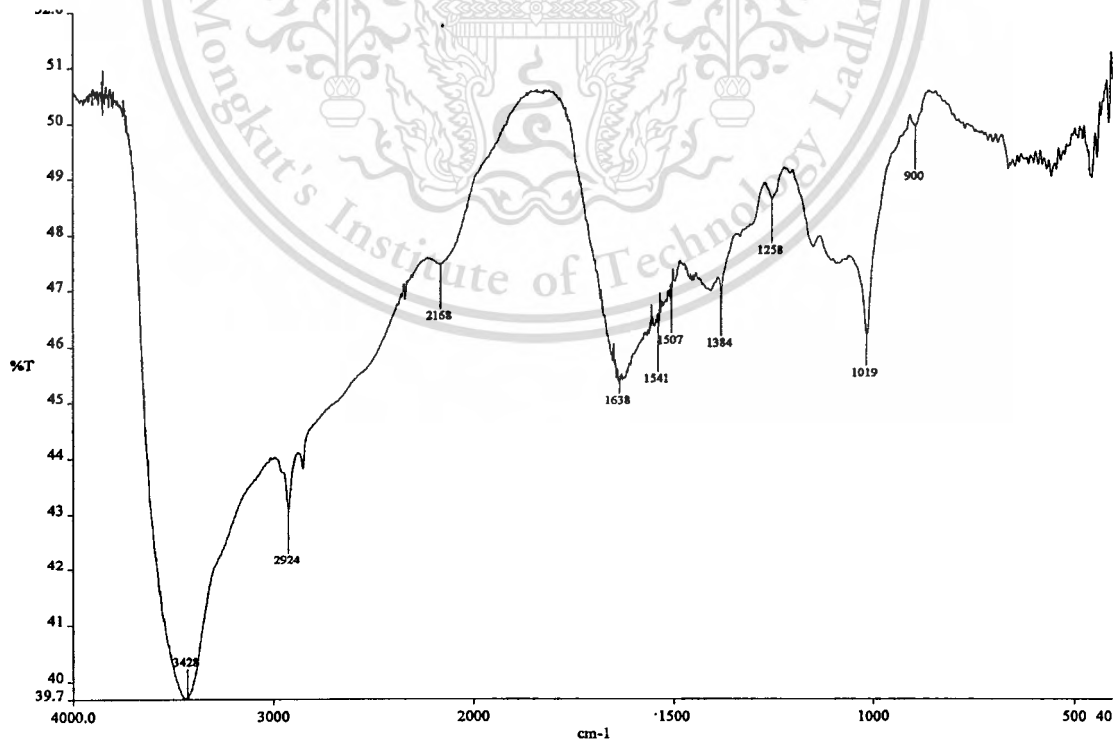

Figure B-10 FTIR spectrum of CMMC3

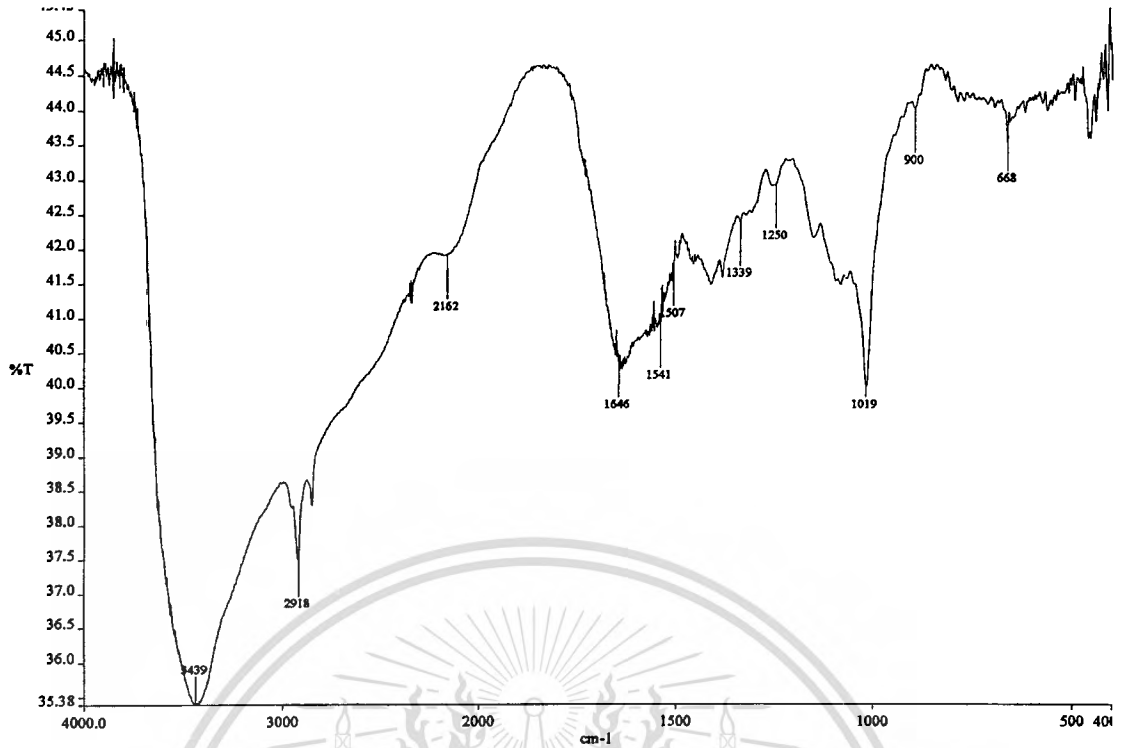

Figure B-11 FTIR spectrum of MMCC3

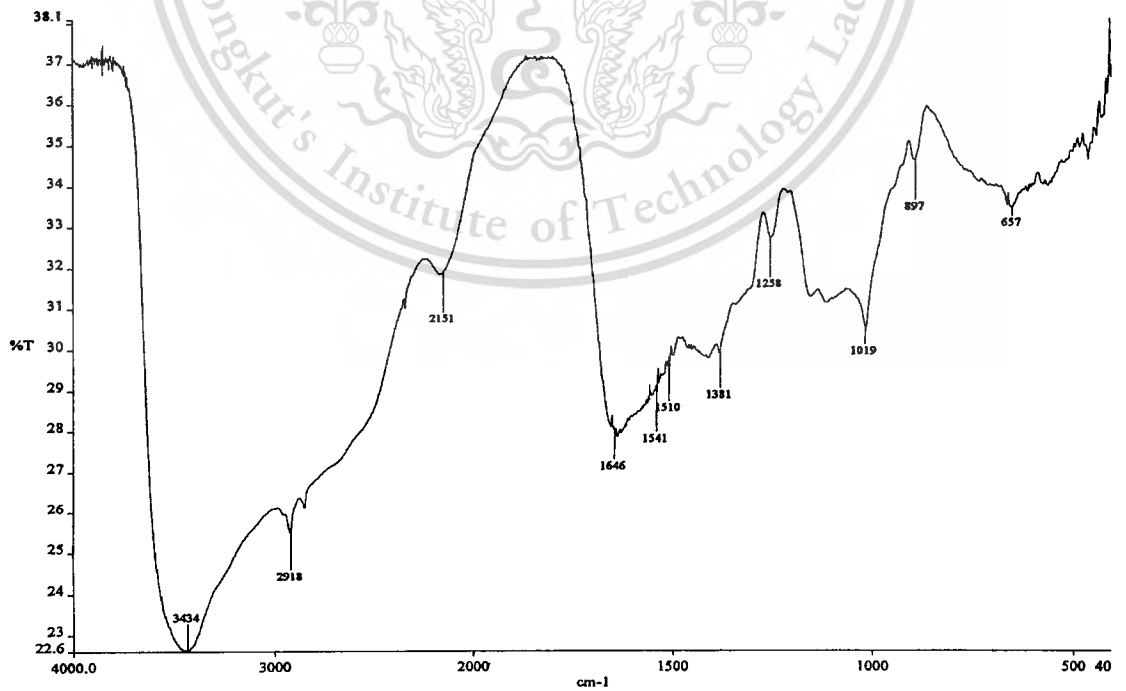

Figure B-12 FTIR spectrum of CCCC

APPENDIX-C

Data of Permeability Test and Slope of Moisture Content/g of Anhydrous Na_2SO_4

Table C-1 Data of permeability test

Sample	Day 0		Day 1	
	W_t (g)	%moisture/ g-Anhydrous Na_2SO_4	W_t (g)	%moisture/ g-Anhydrous Na_2SO_4
Filter paper	95.0498	0.0000	95.1476	0.1029
MMMM1	93.8120	0.0000	93.8331	0.0225
CMMC1	93.2031	0.0000	93.2642	0.0656
MMCC1	92.8746	0.0000	92.9459	0.0768
MMMM2	92.7226	0.0000	92.7409	0.0197
CMMC2	94.0503	0.0000	94.0904	0.0426
MMCC2	94.3454	0.0000	94.4310	0.0907
MMMM3	95.5907	0.0000	95.6059	0.0159
CMMC3	94.5719	0.0000	94.6230	0.0540
MMCC3	95.4984	0.0000	95.5895	0.0954
CCCC	93.8508	0.0000	93.9186	0.0722

Table C-1 (Continued)

Sample	Day 2		Day 3	
	W_t (g)	%moisture/ g-Anhydrous Na_2SO_4	W_t (g)	%moisture/ g-Anhydrous Na_2SO_4
Filter paper	95.2488	0.2094	95.3465	0.3122
MMMM1	93.8556	0.0465	93.8755	0.0677
CMMC1	93.3265	0.1324	93.3886	0.1990
MMCC1	93.0160	0.1522	93.0843	0.2258
MMMM2	92.7598	0.0401	92.7780	0.0598
CMMC2	94.1304	0.0852	94.1756	0.1332
MMCC2	94.5122	0.1768	94.5933	0.2628
MMMM3	95.6210	0.0317	95.6362	0.0476
CMMC3	94.6754	0.1094	94.7298	0.1670
MMCC3	95.6830	0.1933	95.7775	0.2923
CCCC	93.9871	0.1452	94.0538	0.2163

Table C-1 (Continued)

Sample	Day 4	
	W_t (g)	%moisture/ g-Anhydrous Na_2SO_4
Filter paper	93.8958	0.0893
MMMM1	93.8958	0.0893
CMMC1	93.4528	0.2679
MMCC1	93.1547	0.3016
MMMM2	92.7975	0.0807
CMMC2	94.2181	0.1784
MMCC2	94.6731	0.3473
MMMM3	95.6517	0.0638
CMMC3	94.7834	0.2236
MMCC3	95.8731	0.3924
CCCC	94.1227	0.2897

Table C-2 Slope of moisture content/g of anhydrous Na_2SO_4 (filter paper, chitosan coated on filter papers, and CHI-MMT/chitosan composite coated on filter papers)

Sample	Slope (%moisture/g-Anhydrous Na_2SO_4/day)
Filter paper	0.1038
MMMM1	0.0225
CMMC1	0.0666
MMCC1	0.0755
MMMM2	0.0201
CMMC2	0.0442
MMCC2	0.0874
MMMM3	0.0159
CMMC3	0.0556
MMCC3	0.0976
CCCC	0.0723